RI 9306

REPORT OF INVESTIGATIONS/1990



# Arch Canopy Verification Tests

By Richard A. Allwes and C. P. Mangelsdorf

1910 ★ 80 YEARS ★ 1990

BUREAU OF MINES

UNITED STATES DEPARTMENT OF THE INTERIOR

**Mission:** As the Nation's principal conservation agency, the Department of the Interior has responsibility for most of our nationally-owned public lands and natural and cultural resources. This includes fostering wise use of our land and water resources, protecting our fish and wildlife, preserving the environmental and cultural values of our national parks and historical places, and providing for the enjoyment of life through outdoor recreation. The Department assesses our energy and mineral resources and works to assure that their development is in the best interests of all our people. The Department also promotes the goals of the Take Pride in America campaign by encouraging stewardship and citizen responsibility for the public lands and promoting citizen participation in their care. The Department also has a major responsibility for American Indian reservation communities and for people who live in Island Territories under U.S. Administration.

Report of Investigations 9306

# Arch Canopy Verification Tests

By Richard A. Allwes and C. P. Mangelsdorf

UNITED STATES DEPARTMENT OF THE INTERIOR
Manuel Lujan, Jr., Secretary

BUREAU OF MINES
T S Ary, Director

**Library of Congress Cataloging in Publication Data:**

**Allwes, Richard A.**
Arch canopy verification tests / by Richard A. Allwes and C. P. Mangelsdorf.

p. cm. – (Report of investigations; 9306)

Includes bibliographical references.

Supt. of Docs. no.: I 28.23:9306.

1. Mine roof control–Testing. 2. Structural dynamics. I. Mangelsdorf, C. P. II. Title. III. Series: Report of investigations (United States. Bureau of Mines); 9306.

TN23.U43 [TN288] 622 s–dc20 [622'.28] 89-600349
CIP

# CONTENTS



## ILLUSTRATIONS

## ILLUSTRATIONS–Continued



## TABLES



## UNIT OF MEASURE ABBREVIATIONS USED IN THIS REPORT

| | | | |
|---|---|---|---|
| deg | degree | in/s | inch per second |
| ft | foot | kip/ft | kip per foot |
| ft · kip/ft | foot kip per foot | (kip/ft)/ft | kip per foot per foot |
| ft · lbf | foot pound (force) | lbf | pound (force) |
| $ft/s^2$ | foot per square second | $lbf \cdot ft^2$ | pound (force) square foot |
| frame/s | frame per second | pct | percent |
| ga | gauge | rad | radian |
| in | inch | rad/s | radian per second |
| $in^2$/lin ft | square inch per linear foot | s | second |
| $in^3$/lin ft | cubic inch per linear foot | slug/ft | slug per foot |
| $in^4$/lin ft | inch to fourth power per linear foot | V | volt |

# ARCH CANOPY VERIFICATION TESTS

By Richard A. Allwes[1] and C. P. Mangelsdorf[2]

## ABSTRACT

This U.S. Bureau of Mines report presents the results of verification tests conducted on arch canopies constructed of liner plate. Verification tests were conducted to demonstrate the use of the static and dynamic test procedures developed for arch canopies and to establish the validity and conservativeness of the arch canopy design procedure developed by the Bureau. Physical dynamic tests served as the basis for evaluating the design procedure. Actual dynamic response of the arch canopies was compared with their predicted response utilizing the design procedure. The dynamic tests demonstrated that the actual energy absorption capacity of the arch canopies exceeded the predicted capacity from 18.2 to 30.9 pct, for an average conservative error of 23.5 pct. These tests showed that the arch canopies possess more energy absorption capacity than the design procedure allocates and that the design procedure yields conservative designs. The results of the dynamic tests were also used to develop an empirical factor, which relates the energy of impacting loads to the energy absorption capacity of arch canopies. Use of this empirical factor improved the design procedure by decreasing the average conservative error in predicting the energy absorption capacity of arch canopies to 4.6 pct.

[1]Mining engineer, Pittsburgh Research Center, U.S. Bureau of Mines, Pittsburgh, PA.
[2]Civil engineer, Pittsburgh Research Center; faculty member, University of Pittsburgh, Pittsburgh, PA.

## INTRODUCTION

Fifty-six fatalities and thirteen injuries are attributed to rehabilitating high-roof-fall areas using conventional methods of resupport for the years 1966-86 (*1*, pp. 18-21; *2*).[3] The failure of the conventional methods of resupport to protect mine personnel from recurring roof falls precipitated the use of arch canopies for caved mine entry rehabilitation in 1977 (fig. 1).

When an arch canopy is installed in a mine entry for this type of application, its function is to protect mine workers from roof falls and not to stabilize and support the highly disturbed mine entry. Therefore, reasonable sized roof falls that occur should be withstood by the structure without injury to mine personnel. The potential safety problem, which arises with the use of these structures, is that an improperly designed arch canopy may collapse under the impact loading of a roof fall.

The use of arch canopies for protection against roof falls raises two important issues. The first concerns the magnitudes of the static and dynamic loadings that the structures will most likely encounter in the field. The second concerns the design of arch canopies to ensure their safe use. In 1987, the U.S. Bureau of Mines addressed these safety concerns by developing an arch canopy design procedure and by identifying static and dynamic loading criteria (*1*, pp. 21-29).

The design procedure is based on a balance of the energies involved–loss in potential energy of the roof fall and the strain energy absorbed by the structure. When an arch canopy is subjected to an impact loading at its crown and deflects from its unloaded state to maximum crown deflection, the structure absorbs elastic and plastic strain energy. Thus, the loss in potential energy of the roof fall must be equal to the strain energy absorbed by the arch canopy. The energy absorption capacity of an arch canopy can be derived from its resistance function (static load-displacement diagram). The area under the resistance function, which corresponds to a specific crown deflection, represents the amount of energy that an arch canopy is capable of absorbing. The benefit of the energy approach to solving the problem of designing an arch canopy for dynamic loading situations is that once a resistance function is established for a particular structure, the design of an arch canopy is relatively straightforward.

The decision was made at the outset of this research project to conduct verification tests after the development of the design procedure. This in effect would demonstrate the use of the arch canopy design and test procedures, establish the validity and conservativeness of the design procedure, and help ensure a smooth transition of technology from the Bureau to the mining community.

## DESIGN PROCEDURE PRINCIPLES

Before presenting the physical testing procedures and the results of the verification tests, it is important to discuss the principles involved with the development of the arch canopy design procedure. Although some of these principles are presented in a previous publication (*1*, pp. 23-28), it is appropriate to discuss all of these principles for clarification and continuity of this report.

Furthermore, the structural analyses and physical tests conducted to date provide more insight into the static and dynamic behavior of arch canopies. This knowledge serves to further reinforce the use of the principles in the design procedure.

### IDEALIZED MATHEMATICAL MODEL

One of the major problems encountered in the beginning of the project was developing an idealized mathematical model, which would reasonably represent the dynamic response of an arch canopy to impact loading. The following three issues were addressed before an appropriate model was selected: treatment of an arch canopy as a ring or a shell, location of an applied load that creates the most severe deflections, and the potential for an arch canopy to sidesway or buckle during loading.

The first issue is a question of whether an arch should be treated as a ring (two-dimensional structure where only radial deflections vary) or as a shell (three-dimensional structure where radial and longitudinal deflections vary). The consideration of two loading scenarios–point and distributed loads–provides an answer to this question. If a point load is applied to an arch, the directly loaded member (unit length) does not by itself carry the total load. The adjoining members will contribute to the support of the point load. The result is that the arch resists the point load in a three-dimensional manner, as evidenced by the resultant deflections that vary longitudinally as well as circumferentially. One can also rationalize that the deflections are a maximum at the site of the applied load and diminish to zero at a finite longitudinal distance away from the location of the applied load. Alternatively, if a uniformly distributed load is applied to the entire length of an arch canopy, each member must resist its own load independent of the other adjoining members. The deflections for this load case will be the same at every cross section so that the structure can be viewed as resisting the distributed load in a two-dimensional manner. Deflections will only vary radially. Furthermore, it can also be reasoned that a distributed load applied to the entire length of an arch canopy is the worst load case. To clarify this point, consider a distributed load with a length of 10 ft applied to an arch canopy that is 100 ft in length. The

[3]Italic numbers in parentheses refer to items in the list of references preceding the appendixes at the end of this report.

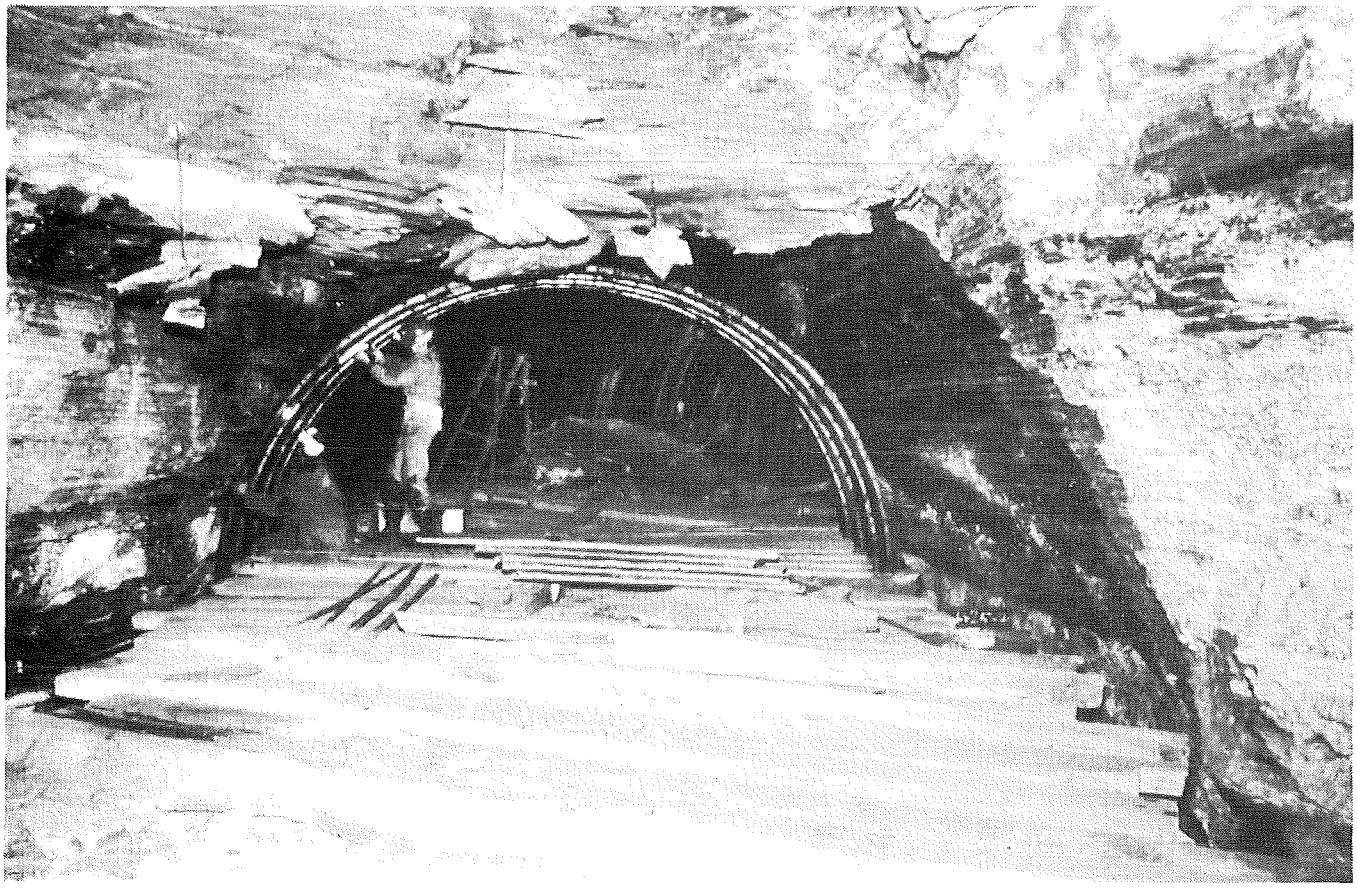

**Figure 1.–Installation of arch canopy for rehabilitation of high-roof-fall area. (Courtesy Camber Corp.)**

most conservative design and worst case loading is to consider the arch to be only 10 ft long. The isolation of the directly loaded members from the adjoining members guarantees a conservative design. As a consequence, the arch will have a considerable reserve of strength. This is because the additional load carrying capacity of the adjoining members is not considered in the overall design. The concept of viewing a load as a distributed (uniform or line) load whose length corresponds to the length of the arch allows the arch canopy to be treated as a ring. For convenience as well as practicality, therefore, all engineering properties for an arch canopy and applied loadings will be expressed in terms of their unit length.

The second issue is the location of an applied distributed load on an arch canopy that will produce the most severe deflections. With respect to the issue of symmetrical (center) versus asymmetrical (off-center) loading,[4] it was assumed in the early stages of this investigation that asymmetrical loading would be less severe for the reason that more energy would likely be required to produce the same vertical deflection for loadings applied at or near the crown. When an eccentric vertical load is applied to a symmetric frame structure, there is a tendency for the structure to shift the load horizontally towards the center. If at the instant of maximum vertical deflection, the structure is still in motion in the horizontal direction, by definition, not all of the energy transmitted to the structure at impact has gone into vertical displacement. Actually, the approximate model one must use to simulate this behavior must possess at least three degrees of freedom as compared with only one for the symmetric case. In addition to translation of the crown in the vertical and horizontal directions, there is a rotational freedom. This is best imagined by thinking of the combined mass of the rock ($M_r$) and the effective mass of the arch canopy ($M_a$) as having a rotational inertia and mounted on a coil spring at the effective center of gravity of the two masses. Since this effective center lies neither at the crown nor at the point of impact, maximum vertical deflection of the crown will not necessarily occur concurrently with the maximum vertical deflection at the point of impact.

Although a mathematical solution to this problem is quite possible, a simple experimental program was conducted at the University of Pittsburgh, Pittsburgh, PA to determine qualitatively the effects of asymmetrical loading.

[4]Loading will imply distributed loading for the entirety of this report unless explicitly stated.

Model arches made of halves of tin cans (approximately 4 in. in diam) were subjected to a line loading tup[5] of standard weight and drop height, but at varying angles away from the crown. Springless, low mass, displacement transducers (LVDT's) were attached to the crown to measure horizontal and vertical motion, and their signals were fed to a two-channel oscillograph running at 4 in/s. Maximum vertical deflection (both dynamic and final) occurred at 0°, while maximum horizontal displacement took place between angles of 25° and 30°. For drops at 10° angles or less (where the rotational effect would be minimal), the maximum dynamic vertical deflection occurred before the arch had begun any significant horizontal motion. For drops involving larger angles, the plastic hinge or crease in the surface associated with the positive bending moment was downhill from the point of impact indicating that the tup rolled or slid relative to the arch. This indicated that the impact was not perfectly plastic (i.e., zero relative velocity during maximum deformation) as assumed in the symmetrical drops. While these limited tests do not verify the assumption that symmetrical loading is the worst condition, they do suggest that, if not, only slightly asymmetrical loading might be worse, but not to a significant degree.

Two asymmetrical dynamic tests were also conducted on full-scale liner plate arch canopies, as will be discussed later in this report. The tests support the premise that an arch canopy subjected to an impact loading at its crown is the worst load case. Until further research or tests prove otherwise, the assumption that symmetrical loadings are most severe in terms of maximum vertical deformations will be used.

The third issue is the question of whether or not an arch will buckle[6] or sidesway when it is subjected to an impact loading at its crown. Early into the project, it was estimated that the distributed load (applied to the crown of an arch) required to buckle an arch in its plane was 1.1 to 2 times the distributed load required to collapse an arch (i.e., sufficient number of plastic hinges[7] to develop in the structure to form a mechanism). This led to the conclusion that an arch canopy will deform symmetrically when it is subjected to static and dynamic loadings applied to its crown. However, static pull tests conducted on model and full-scale arches showed that the structures would sidesway as shown in figure 2. The observed sidesway in all of the static tests is attributed to the asymmetrical formation of plastic hinges.

The reason for the asymmetrical formation of plastic hinges can be explained as follows. When a load is applied to the crown of an arch (with base supports pin connected), a plastic hinge will form at the crown of the arch first because this is the site of the maximum bending moment and thrust. As the load is increased, two more plastic hinges should form ideally at the locations of maximum negative moment simultaneously. Because the load is never precisely at the crown and the arch is never perfectly symmetrical in geometry and material, only one additional plastic hinge forms. As a result, the arch will move laterally (sidesway) in the direction where the additional plastic hinge forms. The arch is on the verge of collapse because a sufficient number of plastic hinges have formed to produce a mechanism.

The observed behavior of the arch canopies under static loading raised the concern that they may sidesway when subjected to impact loading at their crowns. To address this concern, dynamic tests were conducted on model and full-scale arches. For the dynamic tests, a tup was dropped from predetermined heights above the crowns of the arches, and the resultant deformations were measured at various locations. Figure 3 shows an impact test conducted on a full-scale arch and is representative of the behavior observed in all of the dynamic tests. The important observation to be made from this photograph, which was seen in all of the dynamic tests, was that the tendency of the arches to sidesway was suppressed when subjected to impact loadings at their crowns. The vertical momentum of the load caused another plastic hinge to form symmetrically so that lateral movements of the structures were negligible or small in comparison with the large vertical deflections at the crowns.

The problem created by sidesway (fig. 2) is that it occurs at loads less than the ultimate strength the structure would exhibit if lateral displacement at the crown was not permitted. Since lateral displacement did not appear to be significant in all of the early dynamic tests conducted, the presumption was made that the proper resistance of the arch canopy can only be obtained from static tests in which lateral crown displacements do not occur. As a result, the arch canopy was restrained from lateral displacement at its crown so that its static behavior would resemble its dynamic behavior.

The observed minimal lateral movement of the crown of the arches during impact loading and the ability to treat an arch canopy as a ring led to the conclusion that a single spring-mass system could be used to represent the dynamic response of an arch canopy at its crown during impact loading. Structural damping of an arch canopy is not addressed because of its small contribution to energy dissipation during the structure's first quarter cycle of response to impact loading. This decision is warranted when considering the fact that the first quarter cycle of response is the most critical, since this is the period when the maximum plastic deformation occurs in the structure. After the first quarter cycle, damping is an important factor in dynamic structural behavior and would have to be accounted for if the residual structural response was of interest.

The realization that an arch canopy can be treated as a simple oscillator provided the foundation required to

---

[5]Tup is an impacting weight whose length corresponded to the length of the model or full-scale arches.

[6]Buckling of an arch canopy out of its plane is not a consideration because of the lateral restraint offered by the adjoining members of the steel set or liner plate arches.

[7]When the cross section of a steel member totally yields due to the effect of bending with or without axial load, it is termed a plastic hinge. Additional bending deformation can occur without an increase in stress and therefore without increase in resistance. The cross section is then considered a plastic hinge.

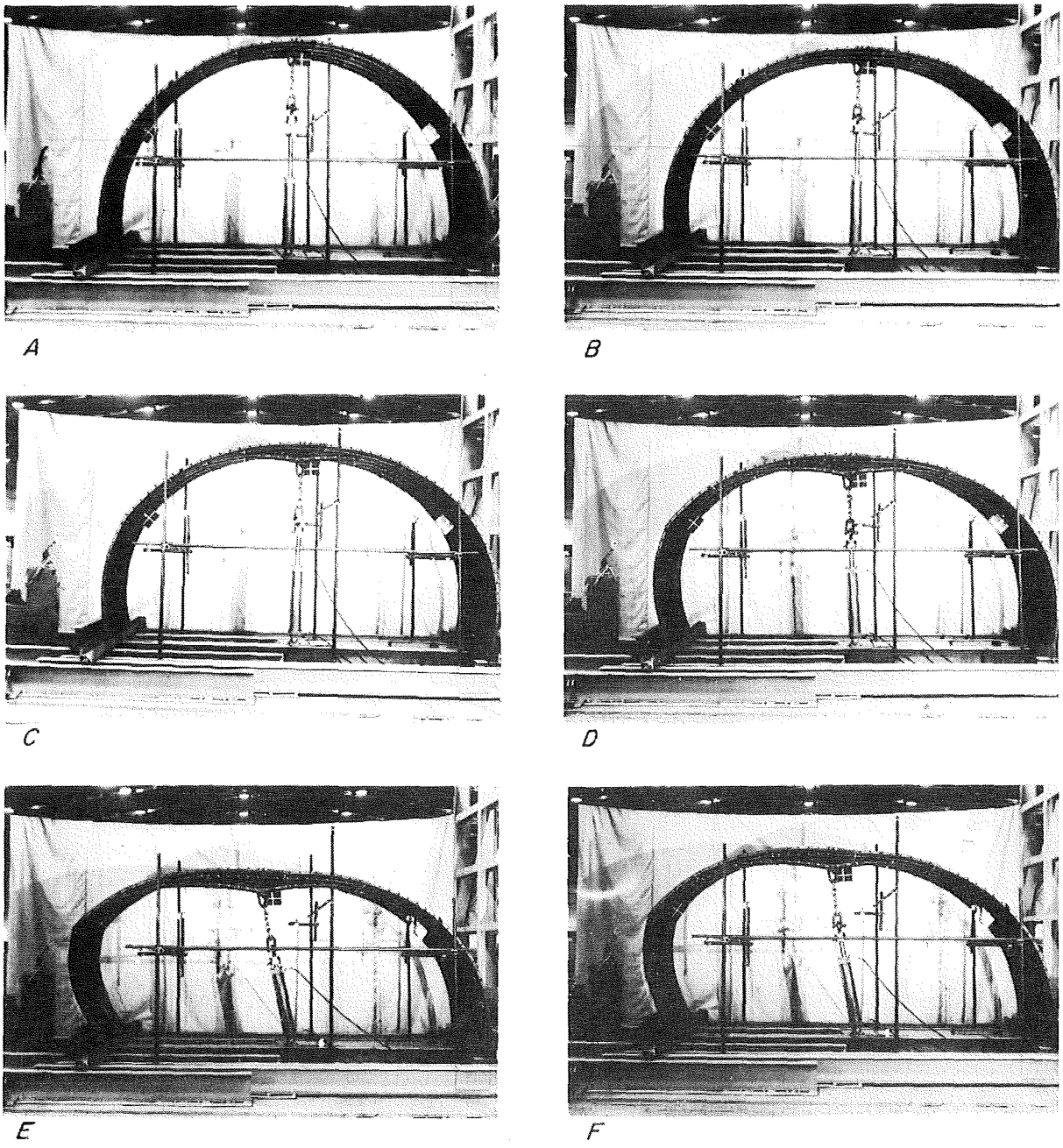


**Figure 2.–Static test.** *A*, **Zero pull force;** *B*, **18.8-kips pull force;** *C*, **19.0-kips pull force;** *D*, **23.3-kips pull force;** *E*, **23.4-kips pull force;** *F*, **pull force released.**

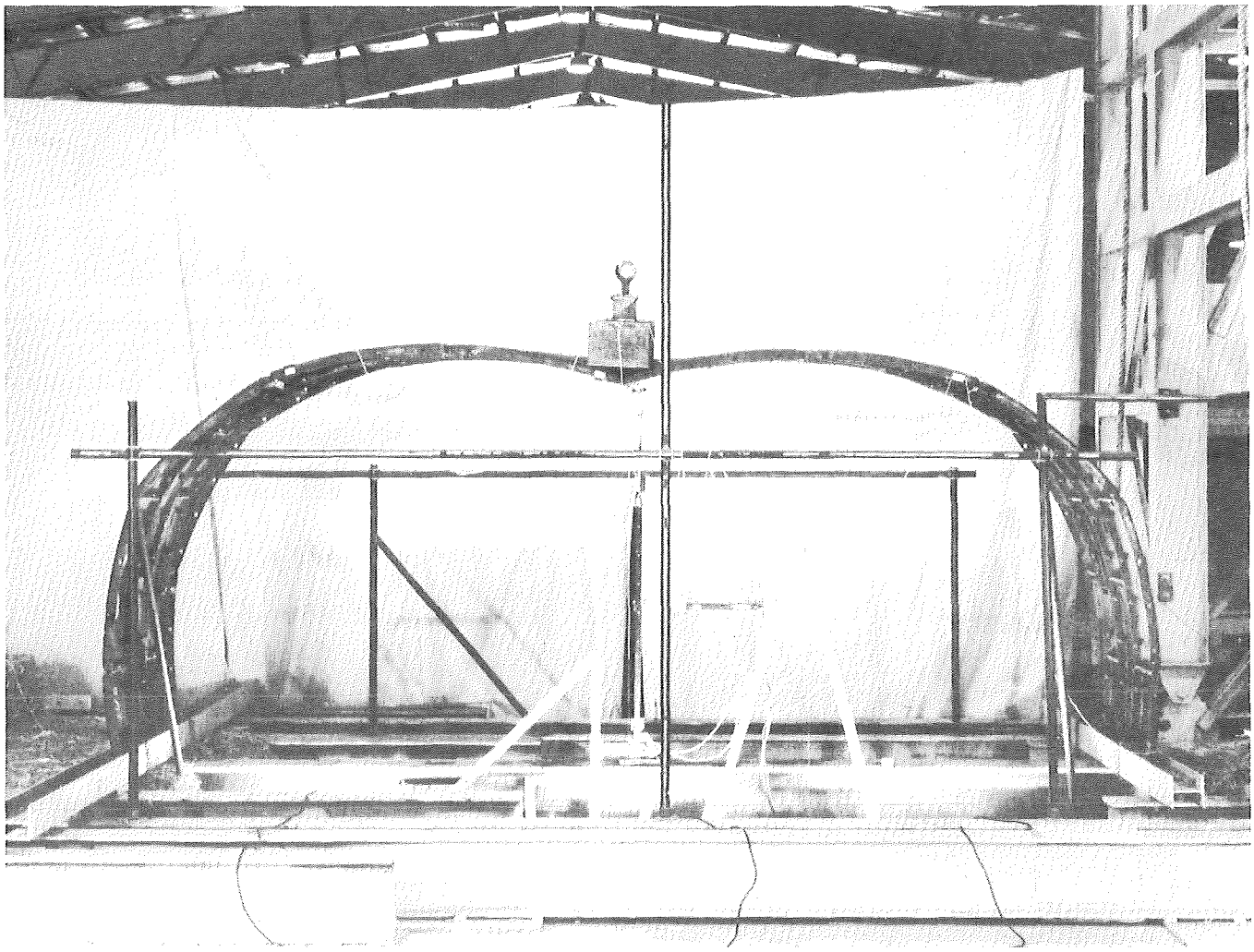

**Figure 3.–Symmetric dynamic test.**

develop a design procedure for arch canopies. The idealized model for an arch canopy is shown in figure 4. The effective mass ($M_a$) of an arch is the mass required to represent its first vertical mode of vibration as a single spring-mass system in simple harmonic motion. The effective mass (slug per foot) will always be less than the actual mass of the arch per linear length. The reason for the difference in mass can be explained by considering the fact that although the frequency of vibration, arch canopy stiffness (K), and maximum deflection must be the same for the two systems, the configuration and distribution of the masses are not. When an arch is vibrating at its first vertical natural frequency, the radial displacements that the differential masses travel vary along the periphery of the arch. The radial displacement at the crown is a maximum, and it is this displacement that the idealized model must undergo when vibrating at the same natural frequency as the arch. Since each differential mass is displacing

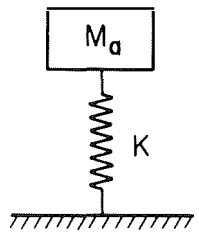


**Figure 4.–Idealized mathematical model of arch canopy–single spring-mass system.**

by different amounts, but at the same frequency, a lumped mass equivalent to the entire mass of the arch cannot be used in the model. This in effect would require each differential mass of the arch to travel the same distance, which is impossible. As a result, the effective mass is always less than the total mass of an arch.

The effective mass can be calculated from the work of Henrych (*3*), a structural dynamics computer program (*4*), Rayleigh's method (*5*), or an experimental method.[8] One consideration in the use of the effective mass for design purposes is that the value obtained is for a structure undergoing elastic deformations, not plastic deformations. The significance of this is when an arch is deformed into its plastic range, the effective mass, frequency, and stiffness of the structure decrease, due to the large geometric changes occurring in the arch. In all of the full-scale dynamic tests conducted to date, the stiffness, frequency, and the effective mass changed for each arch tested. However, the change in stiffness did not account for the total changes in the fundamental frequency of vibration of the structures. Therefore, the effective mass also changed as large plastic deformations occur in an arch. The exact relationship between effective mass and large plastic deformations is not known at this time. However, this problem can be handled empirically using the dynamic test data and this is discussed in a later section in this report.

The stiffness (K) of the model represents the stiffness ((kip per foot) per foot) of an arch and is the relationship between applied load and resultant deflection. Although stiffness is an important design parameter for structures in their elastic range, it is not of significant importance in the arch canopy design procedure because of the large plastic deformations occurring in the arch canopies.

## RESISTANCE FUNCTION

Figure 5 shows a resistance function (crown load-displacement curve) obtained from a static pull test. The resistance function is fundamental to the design of an arch canopy. The presumption made in the early stages of this investigation was that the static resistance function is representative of the dynamic resistance function. All of the dynamic tests conducted support this belief.

Once a resistance function is established for an arch canopy, the resistance (load-carrying capacity) (R) and strain energy absorption capacity ($E_a$) can be determined for specific crown deflections. The area under a resistance function for a given deflection represents the amount of strain energy a structure is capable of absorbing up to that deflection. For an arch canopy, the strain energy occurring during deformation will always be expressed as energy per linear foot for this design procedure. This will allow a comparison to be made between the amount of energy that an arch canopy is capable of absorbing and the energy of a roof fall (foot kip per foot). These two engineering properties, R and $E_a$, are important in the design of an arch. They determine whether or not an arch can carry the static weight and absorb the energy of a roof fall.

[8]The experimental method requires mechanically deflecting and then releasing the crown of an arch and measuring the displacement history as a function of time. The resultant load-displacement diagram obtained when the arch was deflected can be used to calculate the stiffness for the structure. Once stiffness and frequency are known, the effective mass is easily calculated.

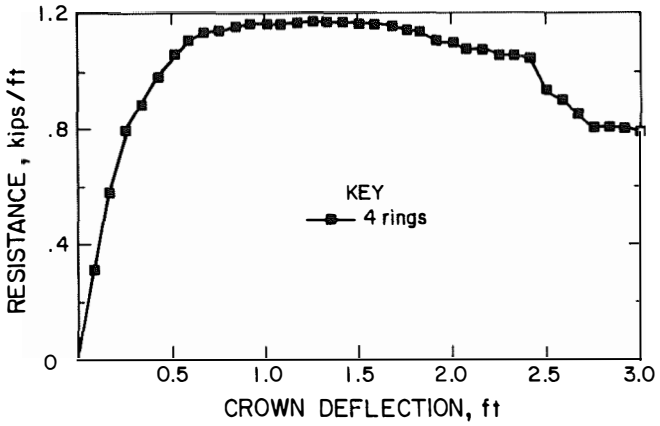


**Figure 5.–Arch canopy crown load-displacement curve.**

A resistance function can be determined for an arch canopy using an elastic-plastic structural analysis. However, the resistance curve obtained from the structural analysis may not be representative of the true behavior of the arch canopy. The predominant reason for the difference between the experimental and analytical curves is that in the structural analysis the abrupt changes in moment of inertia (I) due to the presence of joints cannot be readily accounted for. The joints reduce the flexural rigidity of an arch and its overall stiffness and strength. As a result, the actual resistance function and stiffness will be different than those obtained from a structural analysis.

## PROTECTION HEIGHT

Figure 6 shows the dimensions and notation used for design calculations. The mine operator is responsible for establishing the intended functions for the protected entry. The functional requirements of the entry will dictate the size of the effective area under the arch. The height of the effective area is designated as the protection height ($h_p$). The protection height is an important design parameter because it establishes the minimum clearance of the crown at the time of maximum crown deflection. The void height (H) is the floor-to-roof dimension (after the primary massive roof fall occurs). The height of the arch canopy under consideration is designated as h, and $W_r$ is the weight of roof fall per unit of length expressed in terms of kip per foot.

## LOADING CRITERIA

A study of roof-fall rehabilitation accidents that occurred from 1966 to 1986 led to the development of static and dynamic loading criteria for arch canopies (*1*, pp. 18-24; *2*). Figure 7 shows the cumulative frequency of the kinetic energies of the rehabilitation roof falls. The energies shown in the graph represent the kinetic energies of the roof falls *on impact with the mine floor.* This graph shows that a majority (87 pct) of the roof falls possessed

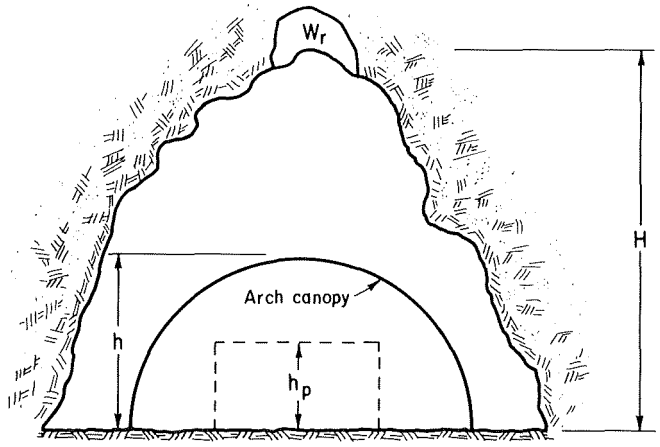


**Figure 6.–Dimensions for design calculations.**

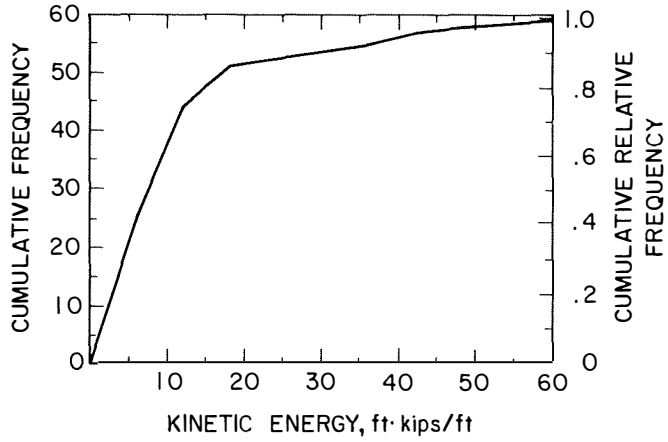


**Figure 7.–Cumulative frequency of kinetic energy of roof falls upon impact with mine floor.**

less than 20 ft·kip/ft of kinetic energy. As can be seen in figure 7, this kinetic energy level represents the point at which the slope of the cumulative frequency graph changes significantly. An argument can be made that this point also represents a reasonable economic constraint for specifying energy absorption requirements for arch canopies. For example, if a mine operator wanted to design an arch canopy to provide protection against 90 pct of the rehabilitation roof falls instead of 87 pct, the energy absorption capacity required of an arch would increase from 20 to 30 ft·kip/ft. This example demonstrates that a 3 pct gain in safety requires a 50 pct increase in energy absorption capacity for the arch. Furthermore, it can also be reasoned that a 3 pct gain in safety will also increase the material costs of the arch by approximately 50 pct.

In view of the facts that a majority of the roof falls possessed kinetic energy levels of less than 20 ft·kip/ft and the diminishing returns associated with designing structures to absorb energy above this level, the decision was made to establish an energy absorption requirement of 20 ft·kip/ft.[9] The implication of this statement is that if an arch canopy is capable of absorbing the energy of a roof fall whose kinetic energy is 20 ft·kip/ft upon impact with the mine floor, then it will be expected to provide protection against at least 87 pct of the roof-fall rehabilitation accidents that occurred from 1966 to 1986.

Once an energy absorption capacity is established for arch canopies, a design energy curve (fig. 8) can be plotted that relates the weight of the rock, $W_r$ (kip per foot), that must fall to create a kinetic energy level of 20 ft·kip/ft on impact with the mine floor. This curve suggests that the greater the void height, the smaller (lighter) the secondary roof falls will be. While this is not strictly true, 87 pct of the roof-fall data referenced above are ≤20 ft·kip/ft.

For purposes of design, the design energy curve provides the necessary static and dynamic loading criteria. The mine operator can calculate from this curve the weight of the roof fall that must drop from a specific void height (the new mine roof height after the primary roof fall occurred) to create an energy level of 20 ft·kip/ft upon impact with the mine floor. This weight represents the maximum static weight that the arch canopy must be capable of supporting. With this in mind, the large geometric changes that occur in the arch during its structural response to impact loading (fig. 3) decrease the static strength of the structure (fig. 5). Therefore, the resistance of the arch at maximum crown deflection ($R_{Ymax}$) (first quarter cycle of dynamic structural response) must be greater than the weight of the roof fall or the structure will collapse. The weight of the roof fall is also used in the calculation of the maximum crown deflection (Ymax) and energy absorption requirement for an arch ($E_a$).

## ENERGY CONSIDERATIONS

The gross energy available for deforming an arch canopy ($E_g$) is the loss in potential energy of the rock fall and the $M_a$ of the arch, namely,

$$E_g = W_r (H-h) + (W_r + g M_a) Ymax, \quad (1)$$

where $E_g$ = gross energy available to deform arch, ft·kip/ft,

$g$ = acceleration due to gravity, 32.2 ft/s$^2$,

$M_a$ = effective mass of the arch canopy; the mass required to represent the arch as a single spring-mass in simple harmonic motion, slug/ft,

and Ymax = maximum crown displacement that occurs during the first quarter cycle of the response of the arch, ft.

[9]The meaning of this statement is that an arch should be capable of absorbing the energy of a roof fall, which would have a kinetic energy level of 20 ft·kip/ft if it was to strike the mine floor. This concept will be further explained in this section of the paper.

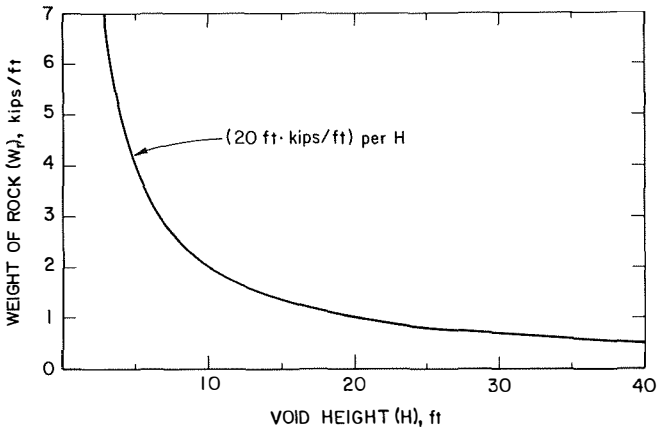


**Figure 8.–Design energy curve.**

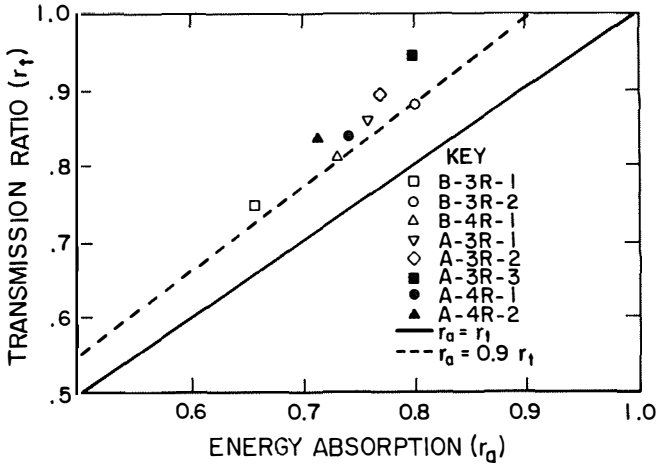


**Figure 9.–Energy absorption ratio ($r_a$) versus transmission ratio ($r_t$).**

Although equation 1 provides an expression for the gross energy available to deform the arch, it does not represent the amount of energy that the arch canopy must be capable of absorbing ($E_a$). The reason for this is that during the impact of the rock fall with the arch, not all of the kinetic energy of the rock fall is transferred to the arch. A portion of the kinetic energy is transformed into noise, heat, local deformation of the rock fall and arch, and the excitation of the natural frequencies of the arch. The expression that relates the transfer of kinetic energy of the rock fall to the arch is called the transmission ratio ($r_t$); it is based on the conservation of momentum and is governed by the equation (*1*, p. 25),

$$r_t = \frac{M_r}{M_r + M_a} \qquad (2)$$

where $M_r$ is the mass of roof fall.

The transmission ratio ($r_t$) is only applicable to the kinetic energy of the rock fall at the instant of impact [the energy given by the expression $W_r$ (H-h) where h is height of arch canopy] and not the gross energy available as given in equation 1. The conclusion can be made that $E_a$ will always be less than $E_g$, due to the loss of kinetic energy of the rock on impact with the arch. The question immediately raised then is, what is the relationship of $E_a$ to $E_g$? It was proposed in the early stage of the project that the ratio of $E_a$ to $E_g$ be greater than a factor that was called the energy absorption ratio ($r_a$). A decision was also made at that time to make $r_a$ equal to $r_t$ until the full-scale physical tests proved otherwise. Eight full-scale impact tests of arch canopies were conducted and these tests showed that $r_a$ is approximately equal to 0.9 $r_t$ (fig. 9). Therefore, a recommendation is made that $r_a$ should be made equal to 0.9 $r_t$. This represents a conservative value for $r_a$ and should only be used for arch canopies that are similar in shape and size to the ones utilized in the dynamic tests. For other types of arches or when the use of the empirical factor 0.9 is in doubt, use $r_t$ for $r_a$.

## CROWN DEFLECTION CALCULATION

The resultant maximum crown deflection (Ymax) during the first quarter of response to impact loading may be obtained from the limit of the inequality relating $E_a$ and $E_g$, namely

$$\frac{E_a}{E_g} \geq r_a, \qquad (3)$$

where $E_g$ is given by equation 1, $r_a$ is obtained from the semiempirical expression 0.91 $r_t$, and $E_a$ is equal to the area under the resistance function up to Ymax for the particular arch canopy under consideration. Ymax must be solved for by an iterative process and is obtained when $E_a$ is equal to 0.9 $r_t$ $E_g$.

## DESIGN CRITERIA

Three criteria must be satisfied in order for an arch canopy to be considered acceptable for a particular rehabilitation project. The first is that the arch canopy must be capable of absorbing the energy of the roof fall by satisfying equation 3. The second is that the weight of the rock fall $W_r$, determined from the design energy curve, must be less than the resistance $R_{Ymax}$ of the arch canopy at the calculated maximum crown deflection Ymax. If this requirement is not fulfilled, the arch will collapse under the static weight of the rock fall. The third is that the maximum crown deflection may not exceed the allowable crown deflection ($h-h_p$).

### DESIGN PROCEDURE

The design procedure is based upon a limiting design energy of less than 20 ft·kip/ft (fig. 8), the weight of the rock fall $W_r$, and designated protection height $h_p$. With these in place, the mining engineer proceeds as follows:

1. By visual observation, determine the void height, H.
2. Using H and the design curve (fig. 8), determine the weight of the rock per linear foot ($W_r$) that must fall to create an energy level of 20 ft·kip/ft if it was to strike the mine floor.
3. Calculate the effective mass ($M_a$) for the arch canopy under consideration using table A-2, if applicable, or another method previously discussed in the report.
4. Using equations 1, 2, and 3, determine if the arch canopy can absorb the energy of the roof fall and calculate the maximum crown deflection (Ymax).
5. Check that $Ymax \leq h\text{-}h_p$.
6. Check that the resistance of the arch canopy at maximum crown deflection ($R_{Ymax}$) is greater than the weight of the rock ($W_r$).

## TEST ARTICLES

The test articles selected for the verification tests were arch canopies constructed of liner plate. Although liner plate arches were used to demonstrate the test procedures and to establish the validity of the design procedure, steel set arches would have been equally suitable.

Two different types of test articles were used and will be designated as test article A (arch A) and test article B (arch B). Test articles A and B were constructed of two- and four-flange liner plate, respectively. Each test article was comprised of three or four rings of liner plate to prevent it from buckling out of its plane, and also to represent reasonably the behavior of the arch canopies.

The configuration of the two-flange liner plate for test article A and its dimensions are shown in figure 10. Each ring was composed of nine liner plates (four 12-Pi and five 16-Pi plates) to form a semielliptical arch. Arch A had a radius of 9 ft 10-9/16 in turning an angle of 194°, a span (width) of 19 ft 7-1/2 in, a rise (height) of 11 ft 5/8 in, and a length of 4-1/2 ft (three rings) or 6 ft (four rings). All of the liner plates were made of a 5-ga material (0.2092-in thick). The plate material and dimensional properties are given in table 1.

The configuration of the four-flange liner plate for test article B and its dimensions are shown in figure 11. Alternating rings were composed of nine 12-Pi plates and eight full and two half 12-Pi plates. The liner plates formed a semicircular arch with a radius of 9 ft, a span of 18 ft, a rise of 9 ft, and a length 4 ft (three rings) or 5 ft 4 in (four rings). All of the liner plates were made of a 5-ga material (0.2092-in thick). The material and dimensional properties of the four-flange liner plate are also given in table 1.

**Table 1.–Properties and dimensions of liner plate**

| Properties and dimensions | 2-flange | 4-flange |
|---|---|---|
| Thickness . . . . . in . . | 0.2092 | 0.2092 |
| Area . . . . . $in^2$/lin ft . . | 3.263 | 1.5818 |
| Section modulus . . . . . $in^3$/lin in . . | 0.0298 | 0.0511 |
| Moment of inertia . . . . . $in^4$/lin in . . | 0.1031 | [1]0.1081 |
| Radius of gyration . . . . . in . . | 0.616 | 0.64 |
| Approx weight, including bolts, lbf: | | |
| 12-Pi full plate . . . . . | 61 | 51.8 |
| 12-Pi half plate . . . . . | NAp | 27.8 |
| 16-Pi plate . . . . . | 79 | NAp |

NAp Not applicable.
[1]Manufacturer recommends for design use 75 pct of the actual radius of gyration given.

## PHYSICAL TESTING PROCEDURES

Arch canopies were physically tested with the use of the impact test structure (ITS). The ITS was designed to provide a versatile frame for the static and dynamic testing of various arch canopy and arch canopy-backfill system configurations (fig. 12). Static tests were conducted by utilizing a hydraulic cylinder, which provided a downward load (pull force) to the crown of the arch canopy. The ITS also accommodates impact testing of arch canopies by the use of a crane-mounted release hook assembly that drops a tup from various heights. [A tup (fig. 3) is an object of significant weight that is dropped from above a test article to create an impact load.] Sidewalls and end walls permit the placement of backfill on the sides or on top of the arch canopies to accommodate testing of arch canopy-backfill systems (soil-structure interaction).

### STATIC TESTS

Static tests were performed on three- and four-ring liner plate arch canopies to establish their elastic and plastic behavior, and also to obtain crown load-displacement diagrams for the structures. These tests also provided a detailed understanding of the failure processes that the arch canopies underwent. As noted previously, the area under a load-displacement curve represents the amount of energy that an arch canopy is capable of absorbing for

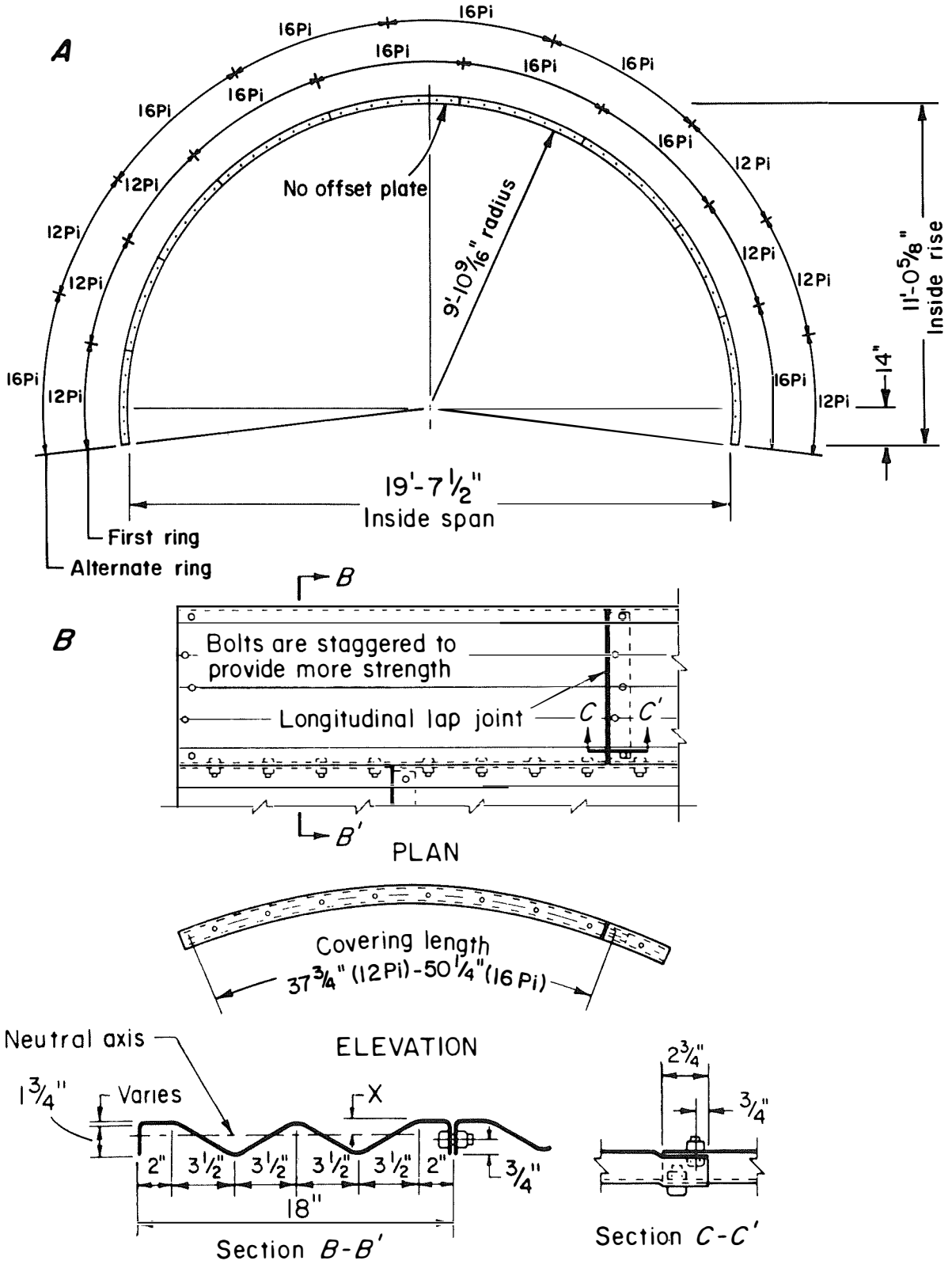


**Figure 10.–Test article A.** *A*, **Configuration;** *B*, **liner plate dimensions.**

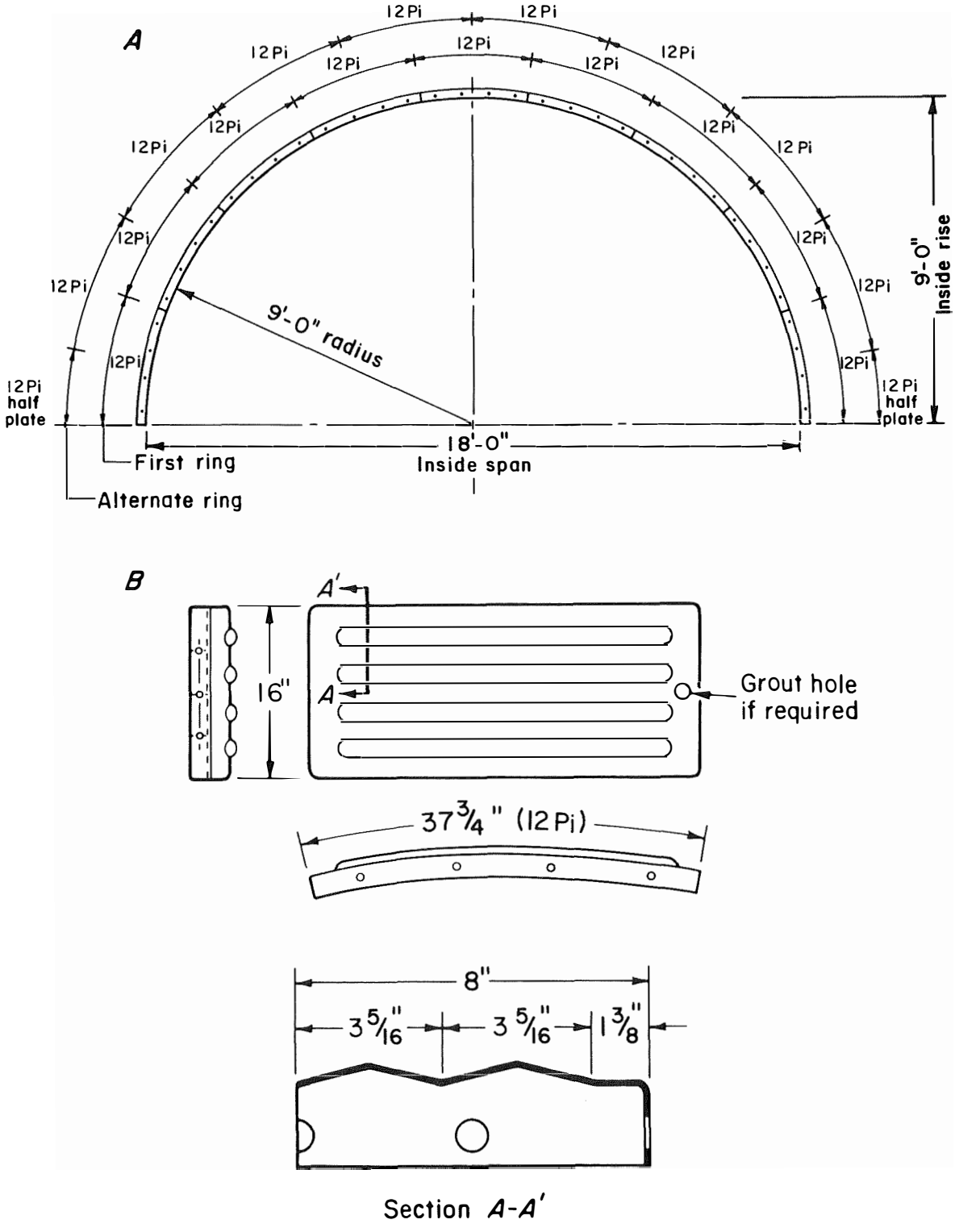


**Figure 11.–Test article B.** *A*, **Configuration;** *B*, **liner plate dimensions.**

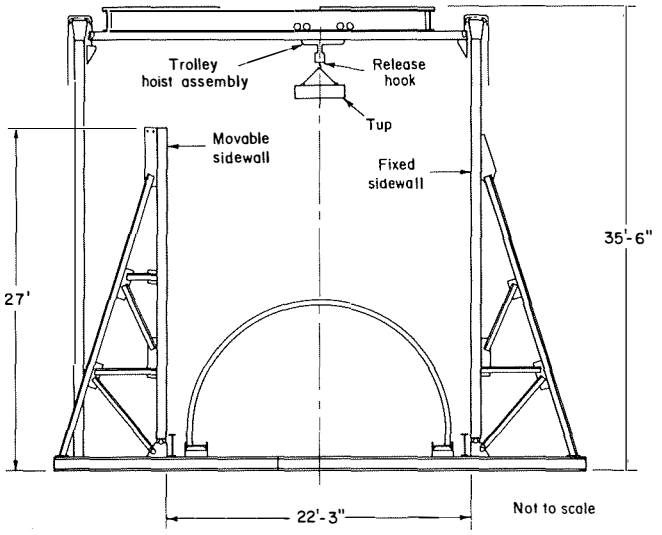


Figure 12.–Front elevation of the impact test structure.

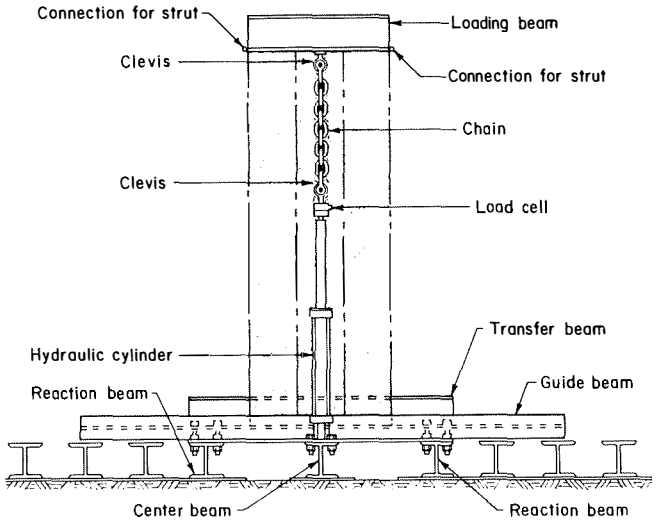


Figure 13.–Schematic of arch installation for static test–side view.

specific crown deflections. The load-displacement curve also shows the amount of resistance an arch canopy is capable of mobilizing for a specific crown deflection. As was discussed earlier in this report, energy absorption capacity and the resistance of an arch canopy are critical parameters in the design of arch canopies for impact loading.

## Test Apparatus

For the static testing of liner plate arch canopies, the pull force of the hydraulic cylinder was distributed along the entire length of the test article at its crown (figs. 13-14). This was done in order to force the structure to behave as a ring (two-dimensional structure) and not as a shell (three-dimensional structure). A loading beam (wide flange beam) was selected so that its center would not deflect elastically more than 1/200th of its length relative to its ends under the maximum loading the arch canopy was expected to carry. The loading beam was also selected to be torsionally stiff enough to prevent its own lateral torsional buckling. Each lip (fore and aft) of the arch canopy was tack welded once to the loading beam to further prevent its lateral movement.

An adjustable strut (with respect to its length) was attached to each lip of the arch to prevent the arch canopy from sideswaying during the static test (figs. 14-15). The arch canopy was restrained from lateral displacement at its crown so that its static behavior would resemble its dynamic behavior.

The arch canopy base supports were restrained against translation, but were free to rotate as shown in figure 14. This was done in order to duplicate the support reactions employed in the field.

## Instrumentation and Data Acquisition System

The installation of the test instruments and data acquisition system are shown in figures 14 and 15. Operation of the equipment was as follows. Hydraulic cylinder (3) exerted a downward force on the crown of the arch, which was transmitted through the load cell (1). A bridge amplifier (2) provided excitation voltage for the load cell and amplified the low-level force signal. Vertical displacement transducers (4) and (5), and the horizontal transducers (6) and (7) produced output signals relating to the position of the arch crown in two dimensions. The 10-V source (9) provided excitation for the displacement transducers while the ± 15-V supply (10) provided power for the buffer amplifiers within the displacement transducers. Connections between the displacement transducers, load cells, voltage supplies, and tape recorder were made at junction box (8). Analog data from each sensor were stored on the magnetic tape recorder (11) for subsequent data processing. The X-Y plotter (12) was connected to the playback of the tape recorder to ensure that the data were going onto the tape during the test.

## Test Conduct

The structure was cycled several times by applying a light load with the hydraulic cylinder. This was done to takeup any play in the system in order to provide a more stable starting position. Following this, the arch canopy was deflected in steps of 3 in by reference to an X-Y plotter. At each 3-in incremental step a photograph was taken of the structure. When the deflection of the structure was approximately equal to one half of the desired maximum crown deflection, the load was slowly released. This was

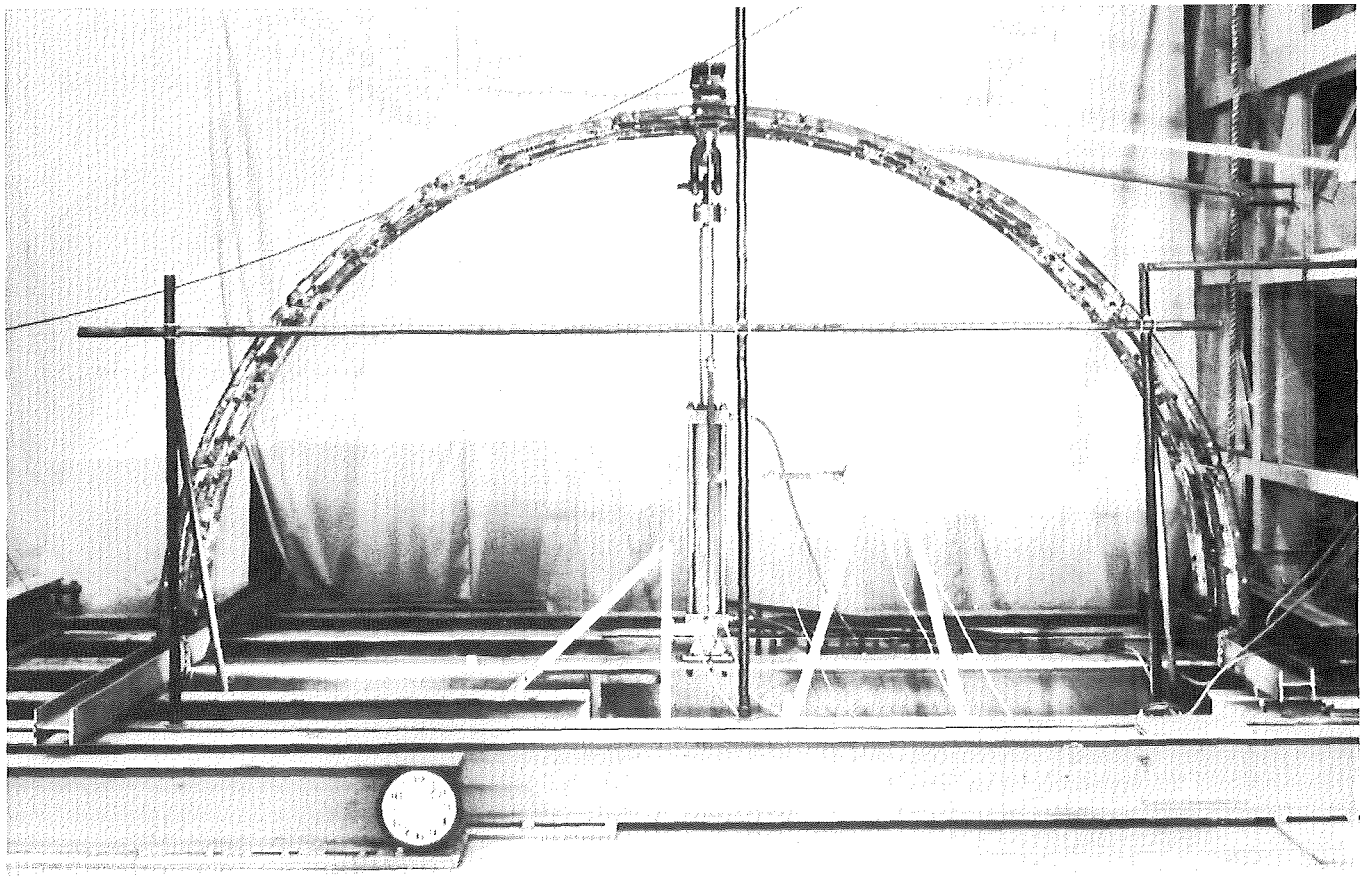

**Figure 14.–Arch canopy installation for static test.**

done to determine the new stiffness of the arch canopy due to the large geometric changes that occurred in the structure. Testing was then resumed at 3-in increments until the desired maximum crown deflection was reached. The load was then slowly released and the static test was terminated.

## SYMMETRIC DYNAMIC TESTS

Symmetric dynamic tests of three- and four-ring liner plate arch canopies were conducted in order to determine their dynamic response to impact loading. A dynamic test involved dropping a tup from specified heights above the crown of an arch canopy and measuring the response (resultant horizontal and vertical crown deflections) of the structure to the impact loading. The measurement of the maximum vertical crown deflection is critical in a dynamic test because it is used to determine the actual energy absorption ratio ($r_a$) and the total amount of energy the arch canopy absorbed during the impact test.

The resistance function established for the particular arch canopy was used in the calculation of the total amount of energy the structure absorbed during the dynamic test. The area under the load-displacement curve, corresponding to the maximum crown deflection measured during the dynamic test, represented the total amount of energy the arch canopy absorbed during the impact loading. Once the energy absorbed by the arch canopy was determined, the actual energy absorption ratio was determined, and the conservativeness of the design was evaluated.

### Test Apparatus

For the dynamic testing of liner plate arches, the impact loads were provided with the use of 1,161-, 2,305.3-, 3,316-, and 3,796-lbf tups. The tups were sized according to weight such that the drop height for the first dynamic test would be at least 6 ft. This was an arbitrarily selected requirement. The uniform weight of the tup is equal to its total weight divided by the length of the test article. The tups were at least as long as the test articles in order to distribute the impact loading along the entire length of the arch canopies and to ensure ring type behavior. The mass of the tup ($M_t$) is equal to its uniform weight divided by the acceleration due to gravity. The arch canopy base supports were restrained against translation, but were free to rotate as shown in figures 3, 12, and 16.

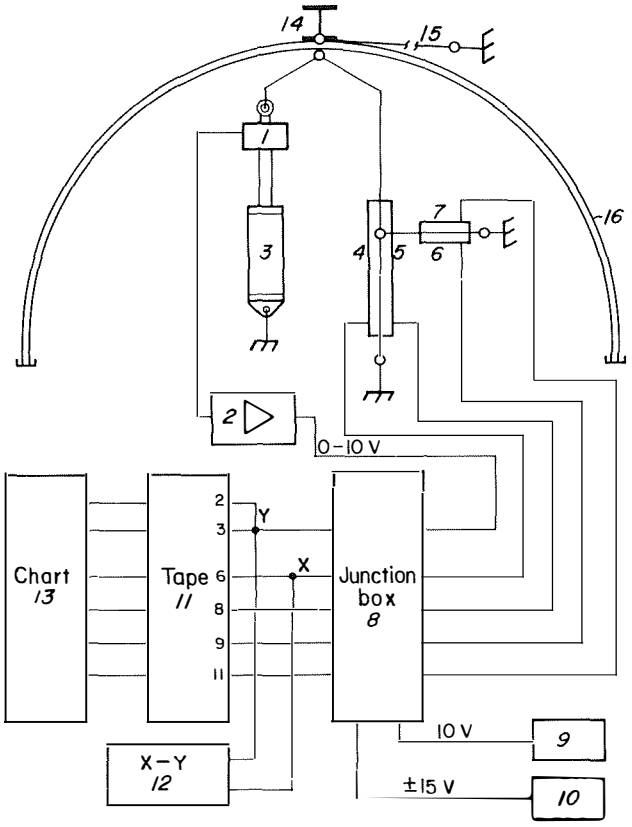


KEY

| | | | |
|---|---|---|---|
| 1 | 20-kip load cell | 9 | 10-V dc voltage source |
| 2 | Strain gauge bridge amplifier | 10 | Plus-minus 15-Vdc power supply |
| 3 | Hydraulic cylinder | 11 | FM magnetic tape recorder |
| 4 | 48-in linear potentiometer | 12 | X-Y plotter |
| 5 | 48-in linear potentiometer | 13 | 8-channel strip chart recorder |
| 6 | 12-in linear potentiometer | 14 | Load distribution beam |
| 7 | 12-in linear potentiometer | 15 | Struts (2) |
| 8 | Junction box | 16 | Test article |

**Figure 15.–Static test instrumentation block diagram.**

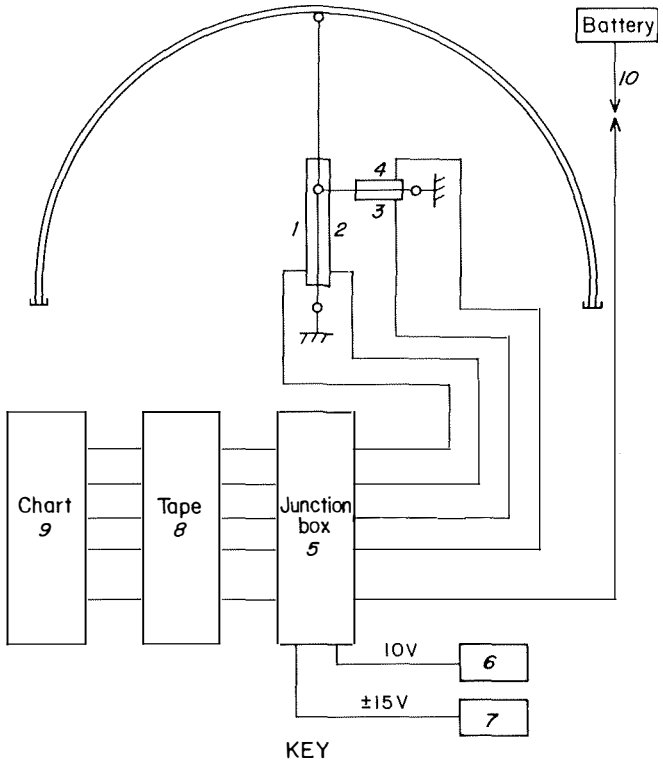


KEY

| | | | |
|---|---|---|---|
| 1 | 48-in linear potentiometer | 6 | 10-Vdc power source |
| 2 | 48-in linear potentiometer | 7 | Plus-minus 15-Vdc power supply |
| 3 | 12-in linear potentiometer | 8 | FM magnetic tape recorder |
| 4 | 12-in linear potentiometer | 9 | 8-channel strip chart recorder |
| 5 | Junction box | 10 | Trigger contact |

**Figure 16.–Dynamic test instrumentation block diagram.**

## Instrumentation and Data Acquisition System

In measuring the dynamic response of an arch canopy, two sets of redundant displacement transducers (fig. 16) were used to ensure accuracy and reliability, since it was quite conceivable that one transducer set could fail during the impact loading. Linear potentiometers were used as displacement transducers because of their ability to respond to large accelerations. (Previous dynamic tests showed that the response of wire-pull transducers were poor and this was attributed to the failure of the reeling mechanism contained in these transducers to retract the wire fast enough to follow the displacement of the arch canopy crown during impact.) It was not certain, however, whether the shock transmitted through the rods of the potentiometers would damage the transducers. The transducers were, therefore, mounted in pairs in both vertical and horizontal positions and special shock isolators were built into the mounting hardware. The weight of the moveable part of the assembly was determined to be 19.53 lbf.

Five channels of data characterizing the behavior of the arch were recorded on magnetic tape. Figure 15 shows a block diagram of the instrumentation and data acquisition setup. Displacement transducers (1), (2), (3), and (4) are used to monitor the movement of the crown in two dimensions. The voltage source (6) provided excitation for the transducers, and the power supply (7) powers the buffer amplifiers within the transducers. The junction box (5) provided a common connection point for the various instruments. The tape recorder recorded the four channels of analog displacement data and one channel of step change voltage (10) derived from a trigger located on the tup. A trigger contact connected to the tup would break after the tup had fallen a predetermined distance, and the resultant step decrease in voltage provided a marker on the tape recorded data and acted as a reference point for data processing. The strip chart recorder (9) was used for real-time data monitoring and also for redundant monitoring of the deflection and trigger signals.

### Test Conduct

Prior to each impact test, the tup was leveled to ensure an even contact between the bottom surface of the tup and the crown of the arch canopy. The tup was then lifted and positioned to the specified drop height above the arch canopy and centered so that the centerline of the tup paralleled the centerline of the arch canopy. A still photograph was taken of the arch canopy before and after each impact test. Just prior to the release of the tup, the tape and strip chart recorders and the high-speed motion camera were started. During the ensuing impact, pictures were taken at a speed of 200 frame/s. The tape and strip chart recorders captured the four channels of displacement data, plus the trigger signal.

Following each impact test, the tup remained on the arch. Displacement data were again recorded as the tup was lifted off of the arch canopy. The resultant elastic spring-back deflection ($\Delta_{st}$) was used to calculate the new stiffness of the structure for the large geometric changes that had occurred in the structure.

## ASYMMETRIC DYNAMIC TESTS

The purpose of the asymmetric dynamic tests was to verify the premise that the worst loading condition that can occur is when a rock fall strikes the crown of an arch. Off-center impact tests on model arches supported this belief, as was previously discussed in this report. However, the question remained as to whether full-scale arch canopies would exhibit similar behavior.

Four-ring liner plate arch canopies served as test articles for the asymmetric dynamic tests. Four rings were used as opposed to three primarily to preserve symmetry in the structure and to negate the influence of the joints within a longitudinal cross section on the location of the plastic hinges developing in the regions of maximum bending moment. The tests consisted of dropping a tup from an identical drop height as was previously used for the symmetric dynamic tests. The two tups used in the tests weighed 2,305.3 and 3,763.2 lbf. Each tup was fabricated so that its bottom surface was tangent to the arch canopy's surface at the impact site. The impact site on an arch canopy was located 10° off-center from its crown (fig. 17). The instrumentation, data acquisition system, and test conduct were identical to those used for the symmetric dynamic tests.

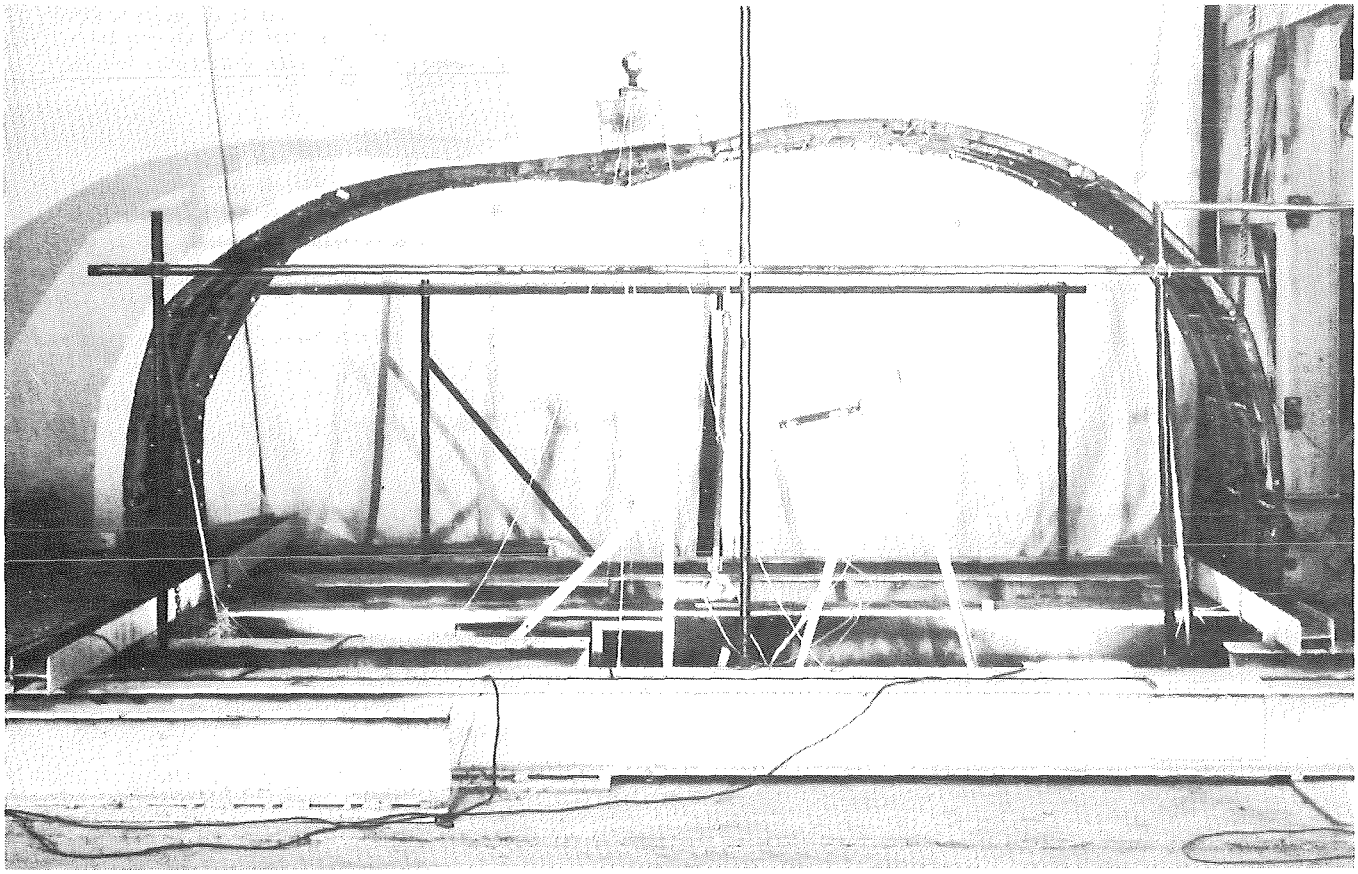

**Figure 17.–Arch canopy deformation due to asymmetric dynamic test.**

# TEST RESULTS

## STATIC TESTS

Figures 18*A* and 19*A* present the results of four static pull tests conducted on two- and four-flange liner plate arch canopies. As previously discussed, the numeric value for resistance is the applied static load divided by the length of the test article. The peak of a curve represents the maximum resistance ($R_m$) that an arch canopy can mobilize against loading and is also indicative that a mechanism has formed in the structure. The portion of the curve to the left of $R_m$ represents the elastic range for an arch canopy and the remainder represents the plastic range. Actually, some plastic action has taken place at the crown by the time $R_m$ has been reached. However, the structure is not yet a mechanism until then.

A comparison of the resistance curves for arch A shows that they are quite similar, except for the last 2 ft of crown deflection (fig. 18*A*). No explanation can be given for the greater load-carrying capacity the three-ring two-flange arch canopy demonstrates at the tail end of the resistance curve. It can only be reasoned that the resistance curve of the four-ring arch canopy is more representative of the actual strength and load-carrying capacity of all two-flange arch canopies of this geometry. This becomes apparent when the influence of the number of joints and full plates that are present when a plastic hinge develops in an arch canopy is considered. A more representative behavior of an arch canopy will be established when the number of joints and full plates in the longitudinal cross section match.

Figure 19*A* shows that the four-ring test article has a greater load-carrying capacity than the three-ring test article. This is attributed mainly to the influence that the number of joints has on the static load required to cause a plastic hinge to form in the structure. In general, an arch canopy should always have an even number of joints within its longitudinal cross section. (Figures 10 and 11 demonstrate that joints and plates are staggered with respect to one another.) It is for this reason that the suggestion is now made that all liner plate arches tested statically or dynamically be composed of an even number of rings and that the minimum number of rings to be used is four.

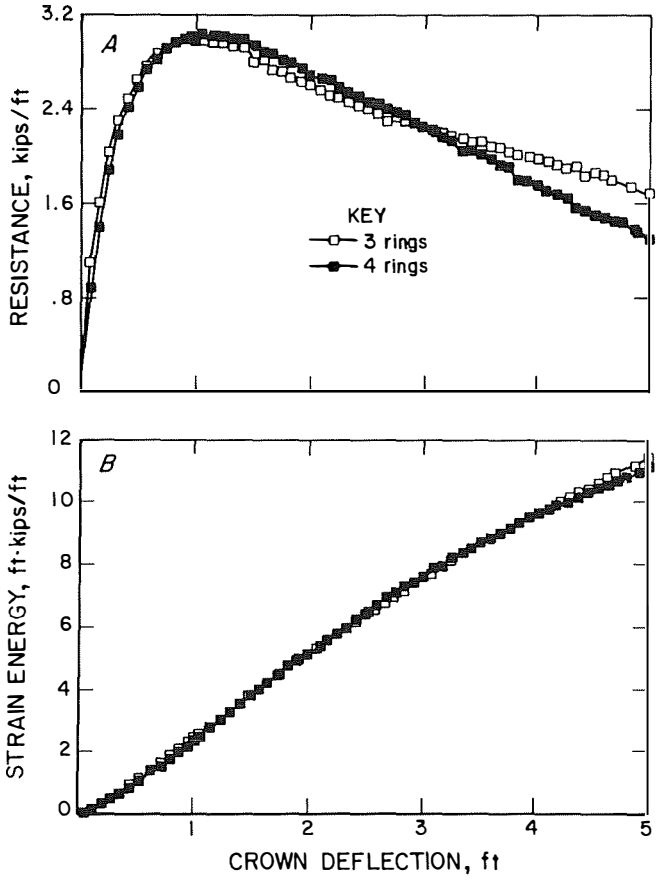


**Figure 18.–Arch A design curves. *A*, Resistance functions; *B*, strain energy curves.**

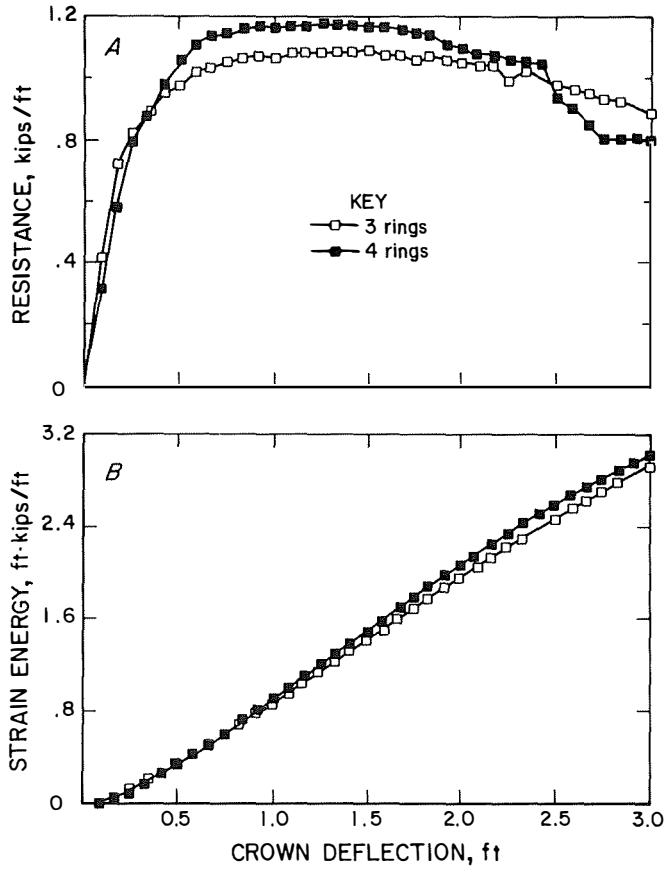


**Figure 19.–Arch B design curves. *A*, Resistance functions; *B*, strain energy curves.**

The sudden loss in resistance of the four-ring arch canopy (fig. 19*A*) was caused by local fracturing and tearing of the liner plate at the crown. The fractures initiated at the bolt holes in the liner plate are the result of large strains the liner plate experienced at the crown.

Strain energy curves are provided in figures 18*B* and 19*B* for all of the arch canopies statically tested. The strain energy curves were obtained from calculating the area under the resistance curves. These curves represent the energy absorption capacity of the arch canopies and are essential for the design of an arch canopy. A comparison of the strain energy curves for the three- and four-ring arch canopies show that they are relatively similar. However, for purposes of design, the energy curves of the four-ring arch canopy should be used.

## SYMMETRIC DYNAMIC TESTS

Table 2 provides all of the design data, test data, and test results for the eight symmetric dynamic tests conducted. Four arch canopies were involved in the tests. Three test articles were subjected to two or three consecutive dynamic tests.

The first section of table 2 provides, the data used for the design of the dynamic tests. The effective masses for the arch canopies were determined with the use of tables 1 and A-1. The drop height for each test was found by solving equation 3 iteratively for Ymax such that $r_t E_g$ or $0.9 r_t E_g$ and $E_a$ balanced. (Use of equations 1 and 3 and the strain energy curve for the appropriate test article allowed the maximum crown deflection (Ymax) for the first quarter cycle of response to be determined.) The energy absorption ratio ($r_a$) was made equivalent to $r_t$ for the first five dynamic tests and involved only the three-ring test articles. The last three dynamic tests conducted incorporated the use of the empirical factor of 0.9, which was derived from data of the previous five dynamic tests.

The middle section of the table provides the actual test data measured. The parameter represents the fundamental period of vibration ($\tau$) for the tup resting on the oscillating arch after the transient vibrations are damped out. The fundamental period of vibration is required to calculate the new effective mass of the arch canopy for a subsequent impact test. The change in effective mass of the arch canopy is a result of the large geometric changes that have occurred.

**Table 2.–Symmetric dynamic tests–design data, test data, and test results**

| Test identification[1] | A-3R-1 | A-3R-2 | A-3R-3 | A-4R-1 | A-4R-2 | B-3R-1 | B-3R-2 | B-4R-1 |
|---|---|---|---|---|---|---|---|---|
| DESIGN DATA | | | | | | | | |
| Tup: | | | | | | | | |
| Total weight, kip | 3.32 | 3.32 | 3.32 | 3.80 | 3.80 | 1.16 | 1.16 | 2.31 |
| Uniform weight, kip/ft | 0.74 | 0.74 | 0.74 | 0.63 | 0.63 | 0.29 | 0.29 | 0.43 |
| Drop height, in | 88 | 60 | 42 | 161 | 75 | 95 | 37 | 71 |
| $M_a$, slug/ft | 3.61 | 2.55 | 1.15 | 3.61 | 3.65 | 2.88 | 1.06 | 2.89 |
| $M'_a$, slug/ft | 3.75 | 2.69 | 1.29 | 3.74 | 3.78 | 3.03 | 1.21 | 3.03 |
| $r_t$ | 0.86 | 0.90 | 0.95 | 0.84 | 0.84 | 0.75 | 0.88 | 0.82 |
| $r_t E_g$, ft·kip/ft | 6.50 | 5.18 | 4.28 | NAp | NAp | 2.44 | 1.22 | NAp |
| $0.9 r_t E_g$, ft·kip/ft | NAp | NAp | NAp | 8.29 | 4.61 | NAp | NAp | 3.05 |
| $E_a$, ft·kip/ft | 6.50 | 5.18 | 4.28 | 8.29 | 4.61 | 2.44 | 1.22 | 3.05 |
| Ymax, ft | 2.53 | 2.59 | 2.49 | 3.29 | 2.77 | 2.48 | 1.48 | 3.00 |
| TEST DATA | | | | | | | | |
| $\tau$[2], s | 0.50 | 0.55 | ND | 0.53 | ND | 0.46 | ND | ND |
| Ymax, ft | 2.12 | 2.05 | 1.93 | 3.19 | 2.49 | 2.09 | 1.23 | 3.08 |
| $\Delta_{st}$, in | 2.19 | 2.78 | 3.74 | 2.30 | 3.40 | 1.81 | 2.10 | 4.13 |
| TEST RESULTS | | | | | | | | |
| $E_g$, ft·kip/ft | 7.23 | 5.37 | 4.08 | 10.89 | 5.75 | 3.11 | 1.30 | 4.19 |
| $E_a$, ft·kip/ft | 5.50 | 4.14 | 3.27 | 8.08 | 4.11 | 2.04 | 0.99 | 3.07 |
| $r_a$ | 0.76 | 0.77 | 0.80 | 0.74 | 0.72 | 0.66 | 0.80 | 0.73 |
| K[3,4], (kip/ft)/ft | 4.04 | 3.18 | 2.36 | 3.30 | 2.23 | 1.92 | 1.66 | 1.26 |
| $M_a$[3,5], slug/ft | 2.55 | 1.15 | ND | 3.65 | ND | 1.06 | ND | ND |
| $M'_a$[3], slug/ft | 2.69 | 1.29 | ND | 3.78 | ND | 1.21 | ND | ND |

NAp Not applicable.
ND Not determined.
[1]First letter specifies test article type, arch A or B; next gives number of rings used; last number designates sequence of tests.
[2]Period of vibration of arch and tup.
[3]New.
[4]K = uniform tup weight divided by $\Delta_{st}$.
[5]Based on equation 4.

Once the maximum crown deflection is established, the actual strain energy $E_a$ absorbed by the structure can be found from a strain energy curve, such as the one provided in figure 18*A*. The static rebound $\Delta_{st}$ (due to removal of tup) is used to determine the new stiffness K for the structure.

The stiffness of the structure decreases significantly as a result of the large geometric changes. This is reflected in the table for each consecutive dynamic test. The stiffness of the structure is important for the consecutive impact tests because it represents the new elastic response of the structure to static and dynamic loading, as shown in figure 20*A*. The two additional linear load-displacement curves are plotted on the original resistance curve for arch A and represent the stiffnesses $K_2$ and $K_3$ for consecutive dynamic tests 2 and 3. Figures 20*B* and 20*C* provide the amount of energy arch A is capable of absorbing for each consecutive dynamic test.

The actual amount of energy each test article absorbed ($E_a$) was determined from the its strain energy curve (original or revised) and the measured maximum dynamic crown deflection. The gross energy available to deform the test articles was calculated using equation 3 for the test articles. The actual energy absorption ratio ($r_a$) was obtained by dividing $E_a$ by $E_g$.

The new effective mass of the test articles following a dynamic test was calculated from the equation (*1*, p. 42)

$$M_a = \frac{K\tau^2}{4\pi^2} - M_t - M_{ta}, \qquad (4)$$

where $M_t$ is the mass of the tup, and $M_{ta}$ is the mass of the transducer assembly divided by the length of the test articles. The results show that for each consecutive test conducted, the test articles progressively became weaker, less stiff, and their effective masses became smaller in magnitude.

A review of the transmission ratios and the energy absorption ratios show that estimating $r_a$ as $r_t$ is too conservative. Therefore, an empirical factor is used to adjust the transmission ratio so that it is more representative of the actual relationship of $E_a$ and $E_g$. Figure 9 shows a plot of $r_t$ versus $r_a$ and curves for $r_a$ equal to $r_t$ and $0.9r_t$. The linear curve demonstrates that the use of the empirical factor of 0.9 is still conservative. Another factor, which contributes to the conservativeness of this procedure, is that the arch canopy will almost always be longer than the roof fall. This ensures that the structure will resist the roof fall in a three- instead of a two-dimensional manner. As a result, the arch canopy will always experience less damage than the design procedure predicts for a given roof fall.

The error between the predicted $E_a$ (using the design procedure and $r_a$ equal to $r_t$) and the actual $E_a$ ranged from 18.2 to 30.9 pct, for an average conservative error of 23.5 pct. The error for predicting $E_a$ using $r_a$ equal to $0.9r_t$ ranged from -0.9 to 12.3 pct, for an average error of 4.6 pct. Likewise, the average error between the predicted Ymax using $r_a$ equal to $r_t$ and the actual Ymax was 22.2 pct. Using $r_a$ equal to $0.9r_t$ improved the average error in predicting Ymax to 3.9 pct. Overall, these errors are conservative and demonstrate the validity and conservativeness of the design procedure.

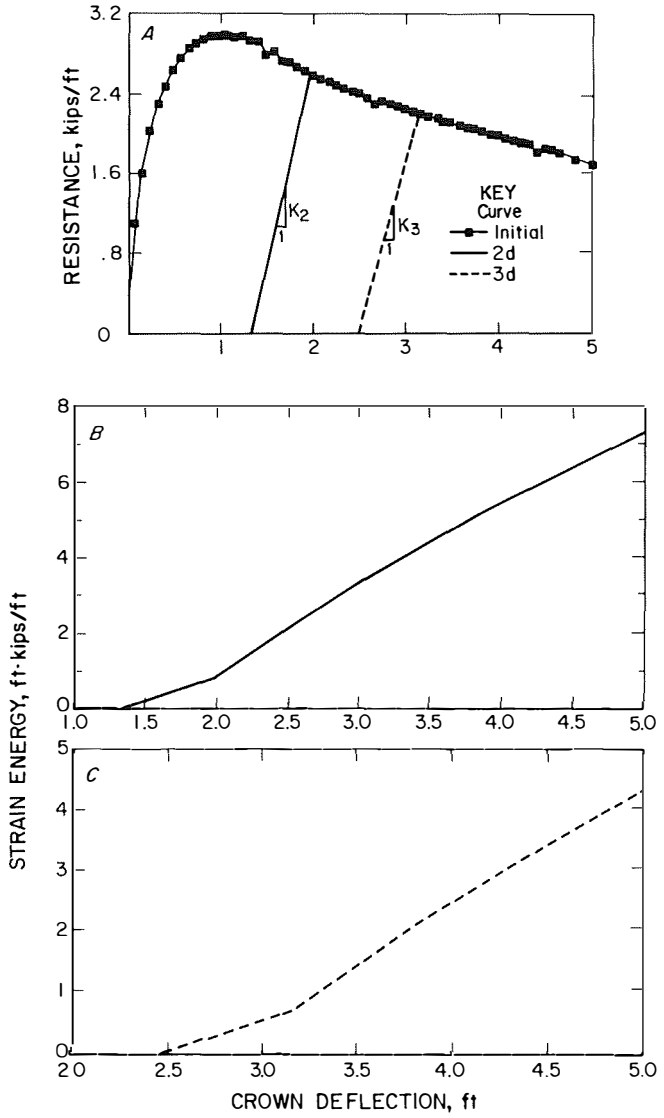


**Figure 20.–Revised arch A design curves. *A*, Resistance function; *B*, strain energy curve 2; *C*, Strain energy curve 3.**

### ASYMMETRIC DYNAMIC TESTS

Two asymmetrical dynamic tests were conducted on four-ring two-flange and four-flange liner plate arch canopies. The tests supported the premise that an arch canopy subjected to an impact loading at its crown is the worst load case. The first asymmetric test consisted of dropping a 3.796-kip tup from a height of 161 in onto a two-flange arch canopy. The impact site was 10° off-center from the crown of the test article (this corresponds roughly to the first set of joints off-center from the crown). This test mirrors the symmetric dynamic test A-4R-1. The resultant maximum crown deflections were 37 in (3.08 ft) vertical and 1.6 in horizontal. A review of table 2 shows that the resultant vertical crown deflection is slightly less than the vertical crown deflection (3.19 ft) for the symmetric dynamic test. The second asymmetric dynamic test involved dropping a 2.3-kip tup from a height of 71 in onto a four-flange arch canopy, which is similar to the symmetric dynamic test B-4R-1. The impact site was also 10° off-center from the crown of the arch canopy. The resultant maximum crown deflections were 26.85 in (2.24 ft) vertical and 1.9 in horizontal. The vertical crown deflection for test B-4R-1 was 3.08 ft. These two asymmetric dynamic tests and the asymmetric tests conducted on model arches support the premise that the worst dynamic load case is a symmetric one.

## CONCLUSIONS AND RECOMMENDATIONS

A design procedure was developed for unbackfilled arch canopies constructed of liner plate and/or steel sets and lagging. Static and dynamic loading criteria were also established for arch canopies. The purpose of the loading criteria and the design procedure is to provide mine personnel with a reasonably conservative method of selecting and designing arch canopies for the purpose of rehabilitating high-roof-fall areas.

Verification tests were conducted on arch canopies constructed of two- and four-flange liner plate. The verification tests served to demonstrate the use of the static and dynamic test procedures developed for arch canopies and to establish the validity and conservativeness of the design procedure. Physical dynamic tests conducted on full-scale and model arches served as the basis for evaluating the design procedure. Actual dynamic response of the arch canopies was compared with their predicted response utilizing the design procedure. The first five dynamic tests demonstrated that the actual energy absorption capacity of the arch canopies exceeded the predicted capacity by an average conservative error of 23.4 pct. The average conservative error in predicting the maximum crown deflection for these tests was 22.2 pct.

The results of the dynamic tests were also used to develop an empirical factor that relates the energy of impacting loads to the energy absorption capacity of arch canopies. Use of this empirical factor improves the design procedure by decreasing the conservative error in predicting the energy absorption capacity of arch canopies to an average of approximately 4.6 pct. Additionally, the error associated with predicting crown deflections was reduced to an average of 3.9 pct. The recommendation is made that the empirical factor $0.9r_t$ should be used for $r_a$ in the energy calculations, as discussed in the report.

## REFERENCES

1. Allwes, R. A., C. P. Mangelsdorf, and D. M. Pappas. Arch Canopy Design Procedure for Rehabilitation of High-Roof-Fall Areas. BuMines RI 9075, 1987, 51 pp.

2. U.S. Mine Safety and Health Administration (Dep. Labor). Roof Fall Fatality Reports, 1983-86.

3. Henrych, J. The Dynamics of Arches and Frames. Elsevier, 1981, 463 pp.

4. Paz, M. Microcomputer-Aided Engineering, Structural Dynamics. Van Nostrand Reinhold, 1986, 351 pp.

5. Timoshenko, S., D. H. Young, and W. Weaver, Jr. Vibration Problems In Engineering. Wiley, 4th ed., 1974, pp. 23-40.

6. Slack, R. L. Structural Analysis. McGraw-Hill, 1948, p. 314.

7. Norris, C. H, and J. B. Wilbur. Elementary Structural Analysis. McGraw-Hill, 1960, 2d ed, pp. 320-327.

8. Flanders, H., R. R. Korfhage, and J. J. Price. A First Course In Calculus With Analytic Geometry. Academic, 1973, pp. 429-432.

# APPENDIX A.–EFFECTIVE MASS OF AN INCOMPRESSIBLE CIRCULAR TWO-HINGED ARCH CANOPY

The effective mass $M_a$ of an arch is the mass required to represent an arch as a single spring-mass system in simple harmonic motion. The Rayleigh Method (*5*)[1] will be utilized in the determination of $M_a$ for an incompressible circular two-hinged arch turning an angle of 2ß (fig. A-1). The effective mass will be calculated from an estimate of the stiffness and frequency of vibration for symmetric deformations of an arch.

The Rayleigh Method is based on the conservation of energy and relates the potential energy of the structure at maximum displacement to its maximum kinetic energy when it is at its equilibrium position. Since the deflections of the arch are mainly attributed to flexural and not axial deformations, the maximum potential energy is equal to the flexural strain energy stored in the structure and the arch is considered to be incompressible. In order to calculate the maximum potential and kinetic energies of the arch, an assumption must be made concerning the shape of the structure at maximum deformation during vibration. It will be assumed that the deflected shape of the arch at maximum displacement can be represented by the static deflection of the structure due to a uniform load (P) applied to its crown (fig. A-2).

The first task is to calculate the vertical and horizontal reactions of the two-hinged arch (fig. A-1) so that the variation of moment around the structure can be determined. The vertical reactions (V) are both equal to P/2, and this is due to symmetry of the loading and the structure. The horizontal reactions (H) are also equal, but cannot be calculated from static equilibrium alone. They can be determined from Castigliano's Second Theorem (*6*), which states that at an unyielding support

$$\frac{\partial U}{\partial H} = 0, \tag{A-1}$$

where $U = \int_0^L \frac{M^2}{2EI}\,dx$, the flexural strain energy, ft · lbf, (A-2)

$H$ = reaction force, lbf,

and $EI$ = flexural rigidity, lbf · ft$^2$.

The moment for the left hand side of the arch (fig. A-1) is

$$M(\alpha) = Hr(\cos\beta - \cos\alpha) + Vr(\sin\beta - \sin\alpha), \tag{A-3}$$

where r is the radius of the arch. Substituting equations A-3 and A-2 into equation A-1, multiplying equation A-2 by a factor of 2, since the use of equation A-3 represents only one-half of the moment variation in the arch, substituting $rd\alpha$ for dx, and changing the limits of integration, yields

$$0 = \frac{2}{EI}\int_0^{\beta} [Hr(\cos\beta - \cos\alpha) + Vr(\sin\beta - \sin\alpha)] * r(\cos\beta - \cos\alpha)\, rd\alpha. \tag{A-4}$$

[1]Italic numbers in parentheses refer to items in the list of references preceding the appendix.

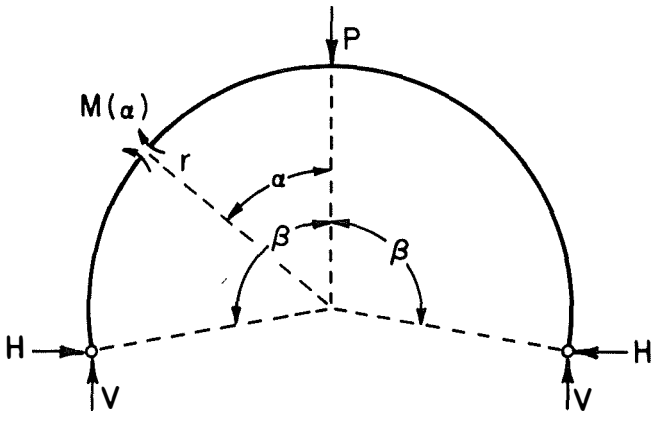


Figure A-1.–Notation for circular arch canopy.

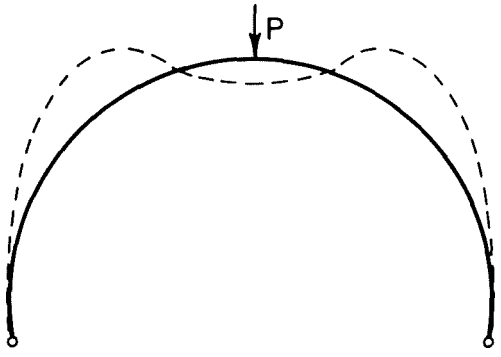


Figure A-2.–Symmetric point load and arch canopy deflection.

Integrating equation A-4 and solving for H as a function of ß gives

$$H(ß) = C_1(ß)P, \tag{A-5}$$

where $C_1(ß) = \frac{1 - 3\cos^2 ß + 2\cos ß(1 - ß\sin ß)}{4\cos ß(ß\cos ß - 2\sin ß) + 2ß + \sin 2ß}$ (A-6)

Once the reactions for the arch are established, the next step is to determine the fundamental frequency of vibration for the symmetric deformation of the structure. The maximum potential energy (*6*, p. 35) of the arch is

$$(PE)_{max} = \frac{1}{2EI}\int_0^{ß} [M(\alpha)]^2 \, r d\alpha. \tag{A-7}$$

The maximum kinetic energy (*6*, p. 36) of the arch is

$$(KE)_{max} = \frac{\rho^2}{2g}\int_0^{L} qw^2 \, dx, \tag{A-8}$$

where q = weight of arch per unit surface area, $lbf/ft^2$,

g = acceleration due to gravity, 32.2 $ft/s^2$,

$\rho$ = frequency of vibration, rad/s,

and w = radial deflection of the arch (ft) due to a concentrated load at the crown.

The moment variation $[M(\alpha)]$ in the left-hand side of the arch is found by substituting equations A-5 and A-6 into equation A-3. The result is

$$M(\alpha) = Pr[C_1(ß)*(\cos ß - \cos\alpha) + \tfrac{1}{2}(\sin ß - \sin\alpha)] \tag{A-9}$$

The principle of virtual work (*7*) will be used to calculate the arch radial deflections. The virtual structure shown in figure A-3 and subjected to a radial virtual unit load will be used in the derivation of the radial deflections. The reaction $\hat{V}_A$ is found from summing the forces in the vertical direction and is equal to $\cos\phi$. The virtual moment variations in the arch for the two arc segments are

$$\hat{M}_1(\alpha) = r[\cos\phi\sin ß - \sin\phi\cos\alpha] \text{ for } 0 \le \alpha \le \phi \tag{A-10}$$

and $$\hat{M}_2(\alpha) = r\cos\phi(\sin ß - \sin\alpha) \text{ for } \phi \le \alpha \le ß. \tag{A-11}$$

The radial deflection $w(\phi)$ is obtained from the equation

$$\hat{1} \cdot w(\phi) = \int_0^{\phi} \frac{M(\alpha)\,\hat{M}_1(\alpha)}{EI} \, r d\alpha + \int_{\phi}^{ß} \frac{M(\alpha)\,\hat{M}_2(\alpha)}{EI} \, r d\alpha \tag{A-12}$$

Substituting equations A-9, A-10, and A-11 into equation A-12 and integrating yields

$$\begin{aligned} w(\phi) = \frac{Pr^3}{EI} \{ & \cos\phi\sin ß[C_1(ß)\,(ß\cos ß - \sin ß) \\ & + \tfrac{1}{2}(ß\sin ß + \cos ß - 1)] - \cos\phi[\frac{-C_1(ß)}{2}(\cos ß - \cos\phi)^2 \\ & + \tfrac{1}{2}(\sin ß(\cos\phi - \cos ß) + \tfrac{1}{2}(\phi - ß) + \tfrac{1}{4}(\sin 2ß - \sin 2\phi))] \\ & - \sin\phi[C_1(ß)*(\sin\phi\cos ß - \frac{\phi}{2} - \frac{\sin 2\phi}{4}) \\ & + \tfrac{1}{2}(\sin\phi\sin ß + \frac{\cos^2\phi}{2} - \tfrac{1}{2})\}. \end{aligned} \tag{A-13}$$

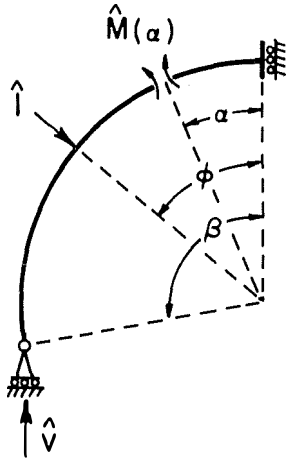


**Figure A-3.–Virtual structure and notation.**

The maximum potential energy for the arch is obtained by substituting equation A-9 into equation A-7. The maximum kinetic energy of the arch is calculated by substituting equation A-13 into equation A-8, changing the limits of integration, and multiplying by a factor of 2 since the limits of integration are only for one-half of the arch. The result is

$$(KE)_{max} = \frac{\rho^2 q}{g} \int_0^{ß} [w(\phi)]^2 \, r d\phi. \qquad (A\text{-}14)$$

Integration of equations A-7 and A-14 is tedious and prone to error. A simpler method is to evaluate the functions $M(\alpha)$ and $w(\phi)$ at each incremental value for $\alpha$ and $\phi$ from 0 to ß, calculate $[M(\alpha)]^2$ and $[w(\phi)]^2$, and integrate $[M(\alpha)]^2$ and $[w(\phi)]^2$ using the trapezoidal rule (*8*). Table A-1 is an excerpt from a spreadsheet and only the values of $[M(\alpha)]^2$ and $[w(\phi)]^2$ evaluated at angles that are multiples of 10° are listed. This table demonstrates the procedure for integrating $[M(\alpha)]^2$ and $[w(\phi)]^2$ for a semicircular arch (2ß is equal to an angle of 180°). For this particular example $C_1$ is equal to $1/\pi$. All angles are referenced to the crown of the arch (figs. A-1 and A-2). The numerical integration for this particular example yields that

$$\int_0^{\frac{\pi}{2}} [w(\phi)]^2 \, r d\phi = r \left[0.000153 \frac{P^2 r^6}{(EI)^2}\right] \qquad (A\text{-}15)$$

and

$$\int_0^{\frac{\pi}{2}} [M(\alpha)]^2 \, r d\alpha = r \, [0.009476 \, (Pr)^2]. \qquad (A\text{-}16)$$

The frequency of vibration may now be calculated by setting equation A-7 equal to A-14 and substituting equations A-15 and A-16 for their respective terms. The circular frequency of vibration is

$$\rho = \left[\frac{61.83 gEI}{qr^4}\right]^{1/2}. \qquad (A\text{-}17)$$

The next step is to recall that the square of the frequency of vibration $\rho^2$ is equal to the stiffness of the structure K(ß) [where the angle ß represents one-half the total angle the radius is turned] divided by its effective mass $[M_a(ß)]$. The stiffness for the arch is equal to the applied load (P) divided by the deflection of the arch at its crown. The deflection of the arch at its crown is the value for w(0°) and can be found in table A-1 as being equal to $0.018942 \cdot (Pr^3/EI)$. The stiffness K(90°) of the arch is P/w(0°). Substituting P/w(0°) for K(90°) and $K(90°)/M_a(90°)$ for $\rho^2$ in equation A-17 and solving for $M_a(90°)$ yields

$$M_a(90°) = \frac{qr}{1.171\, g} \cdot \qquad (A\text{-}18)$$

Equation A-18 represents the effective mass for a semicircular arch. The same procedure may be used to calculate the effective mass for other values of ß or for any arch configuration.

**Table A-1.–Integration of $[M(\alpha)]^2$ and $[w(\phi)]^2$**

| $\phi$ or $\alpha$ | | $w(\phi)$ | $[w(\phi)]^2$ | Cumulative sum of $\frac{\Delta\phi}{2}\{[w(\phi_{i-1})]^2 + [w(\phi_i)]^2\}$ | $M(\alpha)$ | $[M(\alpha)]^2$ | Cumulative sum of $\frac{\Delta\alpha}{2}\{[M(\alpha_{i-1})]^2 + [M(\alpha_i)]^2$ |
|---|---|---|---|---|---|---|---|
| Deg | Rad | $\left[\frac{Pr^3}{EI}\right]$ | $\left[\frac{P^2r^6}{(EI)^2}\right]$ | $\left[\frac{P^2r^6}{(EI)^2}\right]$ | (Pr) | $(Pr)^2$ | $(Pr)^2$ |
| 0 | 0.0000 | 0.018942 | 0.000359 | 0.000000 | 0.181690 | 0.033011 | 0.000000 |
| 10 | .1745 | .016324 | .000266 | .000057 | .099702 | .009940 | .003510 |
| 20 | .3491 | .010149 | .000103 | .000089 | .029876 | .000893 | .004291 |
| 30 | .5236 | .002721 | .000007 | .000097 | .025664 | .000659 | .004337 |
| 40 | .6981 | -.004049 | .000016 | .000098 | .065233 | .004255 | .004743 |
| 50 | .8727 | -.008759 | .000077 | .000106 | .087628 | .007679 | .005809 |
| 60 | 1.0472 | -.010585 | .000112 | .000123 | .092168 | .008495 | .007267 |
| 70 | 1.2217 | -.009334 | .000087 | .000141 | .078715 | .006196 | .008588 |
| 80 | 1.3963 | -.005453 | .000030 | .000151 | .047678 | .002273 | .009331 |
| 90 | 1.5708 | .000000 | .000000 | .000153 | .000000 | .000000 | .009476 |

In order to reduce the computational effort associated with the calculation of $M_a(ß)$, table A-2 contains a list of values for the parameter ($\xi$), which is to be used in the equation

$$M_a(ß) = \frac{qr}{\xi g}, \tag{A-19}$$

where $M_a(ß)$ = effective mass, slug/ft,

$q$ = arch weight per unit surface area, $lbf/ft^2$,

$r$ = arch radius, ft,

and $g$ = acceleration due to gravity, 32.2 $ft/s^2$.

Equation A-19 is only valid for circular, incompressible, two-hinged arch canopies.

The stiffness for a circular arch turning an angle 2ß can be derived for the structure using the principle of virtual work. Figure A-4 shows the virtual structure and unit load placed at the crown. The moment variation, calculated from statics, is

$$\hat{M}(\alpha) = \frac{r}{2}(\sin ß - \sin\alpha). \tag{A-20}$$

The arch crown deflection ($\Delta_p$) due to a uniform load (P) is obtained from the equation

$$\hat{1} \cdot \Delta_P = 2 \int_0^{ß} \frac{M(\alpha)\,\hat{M}(\alpha)}{EI} r d\alpha. \tag{A-21}$$

The integral in equation A-21 is multiplied by a factor of 2 since the integral represents only one-half of the energy stored in the structure. Substituting equations A-9 and A-20 into equation A-21, integrating, and solving for $P/\Delta_p$, which is the stiffness for the structure K(ß), yields

$$K(ß) = \frac{EI}{R^3}\left[\frac{1}{C_1(ß)\,C_2(ß) + C_3(ß)}\right], \tag{A-22}$$

where $C_2(ß) = \cos ß\,(ß\sin ß - 1) + \frac{1}{2}(3\cos 2ß - 1)$, (A-23)

and $C_3(ß) = \frac{1}{2}[\sin ß\,(ß\sin ß + 2\cos ß - 2)$

$$+ \frac{1}{2}(ß - \frac{1}{2}\sin 2ß]. \tag{A-24}$$

Equation A-22 may be used to check accuracy of the stiffness calculated for the structure using the numerical approach. This derived stiffness equation is only applicable for circular arches. The same methodology outlined in this section may be used to calculate the stiffness for an arch of any configuration.

**Table A-2.–Effective masses for circular, incompressible, double-hinged arch canopies**

| ß, deg | $\xi$ | ß, deg | $\xi$ | ß, deg | $\xi$ |
|---|---|---|---|---|---|
| 80 . . | 1.325 | 89 . . | 1.185 | 98 . . . | 1.071 |
| 81 . . | 1.308 | 90 . . | 1.171 | 99 . . . | 1.059 |
| 82 . . | 1.291 | 91 . . | 1.157 | 100 . . | 1.048 |
| 83 . . | 1.275 | 92 . . | 1.145 | 101 . . | 1.037 |
| 84 . . | 1.259 | 93 . . | 1.131 | 102 . . | 1.026 |
| 85 . . | 1.243 | 94 . . | 1.119 | 103 . . | 1.015 |
| 86 . . | 1.228 | 95 . . | 1.106 | 104 . . | 1.005 |
| 87 . . | 1.214 | 96 . . | 1.094 | 105 . . | .995 |
| 88 . . | 1.199 | 97 . . | 1.082 | 106 . . | .989 |

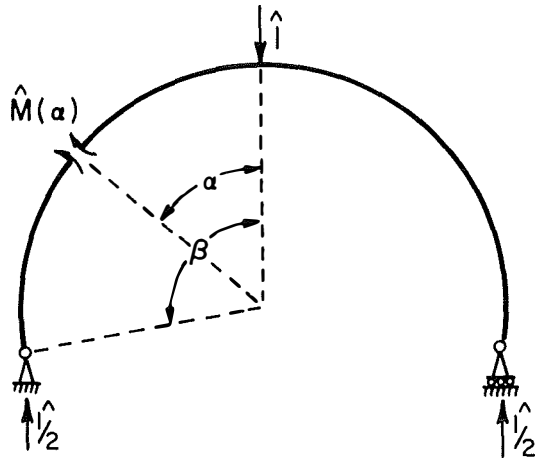


**Figure A-4.–Virtual loads and notation.**

# APPENDIX B.–DESIGN EXAMPLE

A two-flange liner plate arch canopy, arch A, is to be evaluated for a mine entry that experienced a massive roof fall. The new height of the entry, H, is 17 ft. Each ring of the arch is composed of four 12-Pi and five 16-Pi plates (a 12-Pi plate is 37-3/4 in long) (fig. 10). Each liner plate is made of 5 materials (thickness of 0.2092 in). The arch is circular with a constant radius of 118 - 9/16 in turning 193.47° (fig. 10). The weights of the 12- and 16-Pi plates, including bolts and nuts, are 61 and 79 lbf, respectively. Each plate is 18 in wide. A load-displacement curve for this particular arch canopy is shown in figure 18*A* and certain values for this curve are given in table B-1. The elastic and plastic strain energy ($E_a$) stored in the structure for specific crown deflections is also listed in table B-1 and shown in figure 18*B*.

**Table B-1.–Static pull-test data and field evaluation for 17-ft void height**

| Static test | | | Applied energy |
|---|---|---|---|
| Deflection, ft | Resistance, kip/ft | Strain energy, ft·kip/ft | $(0.9r_tE_g)$, ft·kip/ft |
| 0.0 . . . . . | 0.00 | 0.00 | 5.83 |
| .33 . . . . | 2.18 | .43 | 6.18 |
| .76 . . . . | 2.93 | 1.55 | 6.64 |
| 1.08 . . . . | 3.03 | 2.51 | 6.98 |
| 1.52 . . . . | 2.93 | 3.84 | 7.44 |
| 1.93 . . . . | 2.74 | 5.01 | 7.88 |
| 2.33 . . . . | 2.54 | 6.07 | 8.31 |
| 2.68 . . . . | 2.39 | 6.91 | 8.67 |
| 3.11 . . . . | 2.20 | 7.91 | 9.13 |
| 3.50 . . . . | 2.03 | 8.73 | 9.54 |
| 3.91 . . . . | 1.78 | 9.52 | 9.98 |
| 4.33 . . . . | 1.57 | 10.23 | 10.42 |
| 4.67 . . . . | 1.45 | 10.75 | 10.78 |
| 5.00 . . . . | 1.30 | 11.19 | 11.13 |

The weight of the roof fall ($W_r$) that must occur from 17 ft to create an energy level of 20 ft·kip/ft on impact with the mine floor is 1.18 kip/ft, which is determined with the use of figure 8. The protection height ($h_p$) for this particular installation is 6 ft. Since the height of the structure (h) is 11 ft, the allowable maximum crown deflection during the structure's first quarter cycle of response to impact loading is 5 ft ($h-h_p$).

The next step involves calculating the effective mass ($M_a$) for the arch canopy. Equation A-19 and tables 1 and A-2 provide the necessary information for the calculation of $M_a$. For ß equal to 96.7°, $\xi$ is interpolated to be equal to 1.085. The weight of the liner plate per radial length and unit width for this particular example is

$$q = \frac{4 * 61 \text{ lbf} + 5 * 79 \text{ lbf}}{(18 \text{ in})(193.47°)(\pi/180°)(118 - 9/16 \text{ in})} * 144 \frac{\text{in}^2}{\text{ft}^2}$$

$$= 12.8 \text{ lbf/ft}^2.$$

Given that q = 12.8 lbf/ft², g = 32.2 ft/s², and R = 9.88 ft, the effective mass ($M_a$) is determined to be 3.27 slug/ft using equation A-18. The next step is to calculate the transmission ratio, $r_t$ (equation 2). The transmission ratio is calculated to be 0.92. Therefore, the energy absorption ratio ($r_a$) is 0.826 ($0.9r_t$).

Once H, $W_r$, $h_p$, h, $M_a$, $r_a$, and a resistance function are established for an arch canopy; equations 1 and 3 and the resistance function may be used to evaluate the ability of the arch to absorb the energy of the roof fall. The values for $E_a$ and $0.9r_tE_g$ are tabulated in table B-1 and shown in figure B-1. A review of table 1 and figure B-1 reveals that the arch canopy can absorb the impact loading of the roof fall since the values for $E_a$ and $r_a E_g$ are equal for a crown deflection equal to approximately 4.8 ft. The next step is to check that Ymax equal to 4.8 ft is less than or equal to $h-h_p$, and it is. Finally, the resistance of the arch at maximum crown deflection ($R_{Ymax}$) must be greater that the static weight of the roof fall ($W_r$) or the arch canopy will collapse under the static weight of the roof fall. The resistance of the arch at 4.8 ft is 1.41 kip/ft. Therefore, the arch canopy can support the static weight of the roof fall (1.18 kip/ft). The conclusion may now be made that the arch canopy can be used in the mine and that it will provide protection against at least 87 pct of the roof falls that occurred from 1966-1986.

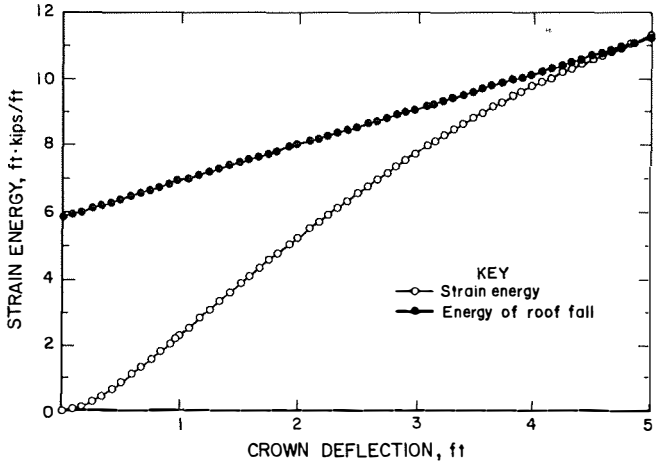


**Figure B-1.–Energy balance diagram.**

## APPENDIX C.–SYMBOLS AND ABBREVIATIONS USED IN THIS REPORT

| | |
|---|---|
| $\Delta_p$ | vertical arch canopy crown deflection |
| $\Delta_{st}$ | vertical static rebound of crown of an arch canopy |
| E | modulus of elasticity |
| $E_a$ | strain energy absorption capacity for an arch canopy |
| $E_g$ | gross energy available to deform an arch canopy |
| g | acceleration due to gravity |
| H | void height or the horizontal base reaction of an arch canopy |
| h | height of arch canopy |
| $h_p$ | protection height |
| I | moment of inertia |
| K | arch canopy stiffness |
| L | length |
| M | moment |
| $M_a$ | effective mass of the arch canopy |
| $M_a'$ | effective mass of an arch canopy and mass of transducer assembly |
| $M_r$ | mass of roof fall |
| $M_t$ | mass tup |
| $M_{ta}$ | mass of transducer assembly |
| P | uniform load applied to crown of an arch canopy |
| Pi | used in reference to the length of liner plate, where Pi is equivalent to 3.14 in |
| $\pi$ | pi |
| q | weight of arch per unit surface area |
| R | resistance (load-carrying capacity) for an arch canopy at a specific crown deflection |
| $R_m$ | maximum resistance of an arch canopy |
| $R_{Ymax}$ | resistance of an arch canopy at maximum crown deflection |
| r | arch canopy radius |
| $r_a$ | energy absorption ratio |
| $r_t$ | transmission ratio |
| $\rho$ | circular frequency |
| $\tau$ | period of vibration |
| U | flexural strain energy |
| V | vertical base reaction of an arch canopy |
| $W_r$ | weight of roof fall |
| w | radial arch deflection |
| $\xi$ | effective mass parameter for an arch canopy |
| Ymax | maximum crown displacement of an arch canopy |
| $\partial$ | partial derivative |

U.S. Department of the Interior
Bureau of Mines
2401 E Street, N.W., MS #9800
Washington, D.C. 20241